Projections of Future CO_2

I.G. Enting and K.R. Lassey
with Appendix by R.A. Houghton

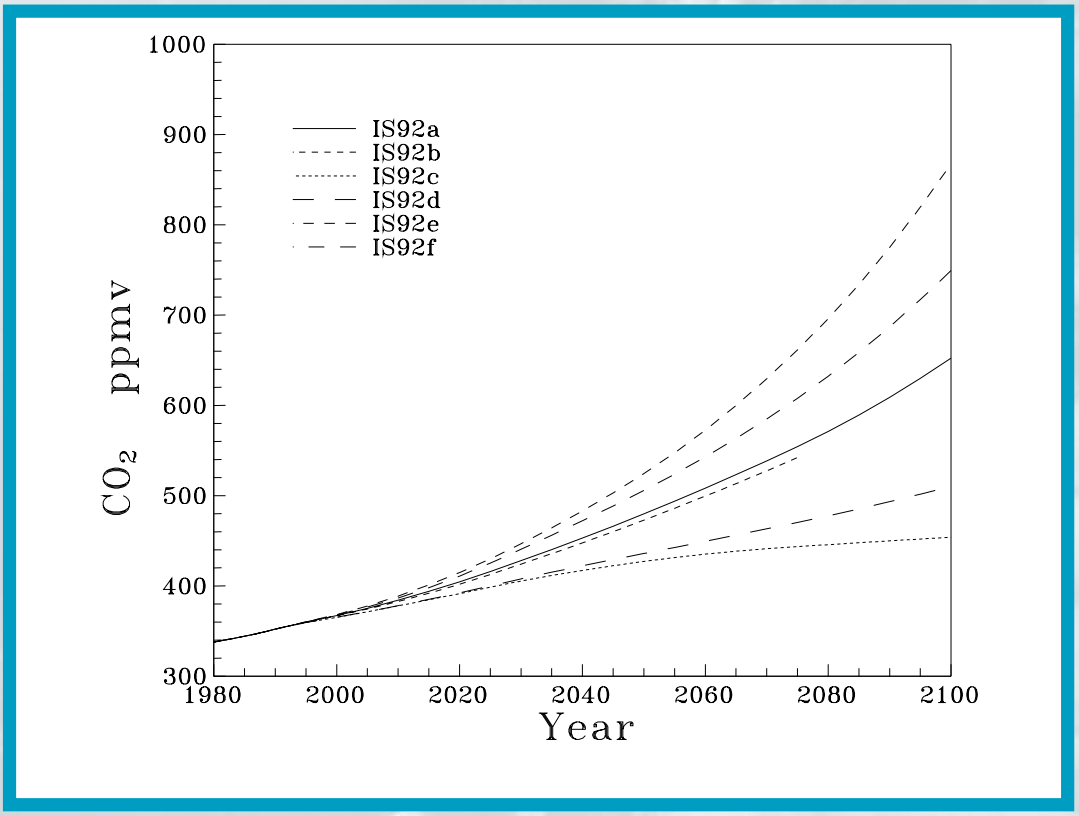

CSIRO

NIWA
Taihoro Nukurangi

CSIRO Division of Atmospheric Research Technical paper no. 27
National Institute of Water and Atmospheric Research NIWA/Atmos/R/93–001

Projections of Future CO_2

I.G. Enting and K.R. Lassey
with Appendix by R.A. Houghton

CSIRO Division of Atmospheric Research Technical paper no. 27
National Institute of Water and Atmospheric Research NIWA/Atmos/R/93–001

National Library of Australia Cataloguing-in-Publication Entry

Enting, I.G.
Projections of Future CO_2

Bibliography.
ISBN 0 643 05252 6 (print edition)
0 643 06638 1 (electronic edition)

1. Atmospheric carbon dioxide – Mathematical models. 2 Climate changes – Mathematical models. 3. Atmosphere – Research.
I. Lassey, K.R. (Keith Richard). II. CSIRO, Division of Atmospheric Research. III. National Institute of Water and Atmospheric Research (NZ). IV. Title (Series: Division of Atmospheric Research Technical Paper; no. 27).

551.5112

Address and contact details: CSIRO Atmospheric Research
Private Bag No.1 Aspendale Victoria 3195 Australia
Ph: (+61 3) 9239 4400; fax: (+61 3) 9239 4444
e-mail: chief@dar.csiro.au

CSIRO Atmospheric Research Technical Papers may be issued out of sequence.

Projections of Future CO_2

I.G. Enting† and K.R. Lassey‡
with appendix by R.A. Houghton¶
† CSIRO, Division of Atmospheric Research.
Private Bag 1, Mordialloc, Vic., 3195. Australia.
‡ Atmospheric Division,
National Institute of Water and Atmospheric Research.
P.O. Box 31-311, Lower Hutt, New Zealand.
¶Woods Hole Research Center
P.O. Box 296, Woods Hole,
Massachusetts 02543, U.S.A.

Abstract

A box-diffusion model is used to calculate the projected atmospheric CO_2 concentrations resulting from the various emission scenarios proposed in the 1992 IPCC supplementary report. The terrestrial biota are treated in terms of a release from land-use change and an uptake from enhanced growth so that (a) the contemporary budget balances (b) the treatment of the biota in the past is consistent with the approach used in the projections. We refine the modelling by making use of ^{14}C data to recalibrate the model and translate the calibration uncertainty into estimates of the uncertainties on the projections. We analyse the projections under a range of assumptions that reflect the uncertainties in the current atmospheric carbon budget. We find that the range of uncertainty implies an uncertainty of about $\pm 15\%$ in the predicted change in CO_2 concentrations between 1990 and 2100.

1. Introduction

The observed increases in the atmospheric concentrations of the so-called greenhouse gases such as CO_2 and CH_4 have caused considerable concern because of the radiative effects of these gases. In order to assess the implications of these increases, an extensive review of the science has been coordinated by the Intergovernmental Panel on Climate Change (IPCC) and the results published in a major report (IPCC, 1990) followed by a more recent update (IPCC, 1992).

The starting point for analysing future global change is a time series, a *scenario*, of plausible future greenhouse gas emissions. From such scenarios, *projections* of future atmospheric concentrations can be calculated using a geochemical model, and from these concentrations, projections of future climate change can be calculated using a climate model. The present report describes a new set of projections of future CO_2 concentrations. These revise earlier projections (Enting, 1991; IPCC, 1990) in several ways. Firstly, we use a new set of release scenarios from

the IPCC (1992) report (see our Figure 1 and appendix A). Secondly, and probably most importantly, we improve the internal consistency of the way in which biomass change is modelled. Finally we present an improved uncertainty analysis.

The CO_2 concentrations calculated from the model are termed 'projections' and not 'predictions' since they are contingent on particular release scenarios. An important part of the analysis is the consideration of a range of scenarios so that the effects of putative courses of action can be assessed.

Geochemical models have been used for many years to project CO_2 concentrations into the future (see for example Siegenthaler and Oeschger, 1978). A number of studies have compared the projections from a range of models (e.g. Emanuel et al., 1985). The IPCC (1990) report consolidated the results of a range of modelling calculations using releases specified as a set of standard scenarios. These were the 'policy' scenarios (derived from considerations of energy-use given a range of response strategies) and 'science' scenarios (designed to explore the response of the carbon system to a wider range of inputs specified in precise mathematical terms).

A major weakness of many (if not all) of the calculations presented in the IPCC (1990) report was the lack of a consistent treatment of the terrestrial biota. The inconsistency had two origins. Firstly, the role of the biota is quantitatively uncertain. Secondly, the specifications of the 'science' scenarios as mathematical functions were unrelated to processes. This effectively precludes a matching of the assumptions about the past and future in a consistent manner. A recent study by Wigley and Raper (1992) has addressed this issue of consistency. Wigley and Raper suggest that the calculations reported in the IPCC (1990) report used models that did not balance the current carbon budget. For models run in 'inverse mode' this is an inaccurate description of the problem — the difficulty is that such models achieve carbon balance in a way that is not necessarily consistent between the past and the future.

The calculations in the IPCC (1990) report did not include an assessment of the range of uncertainty. We present such an analysis. Our uncertainty analysis is undertaken as part of the model calibration procedure. The reason for this is that the specific sensitivity to individual model parameters is less important than the sensitivity to those sets of parameter variations that retain consistency with the observational data. The main data used to calibrate the model are records of atmospheric CO_2 and $^{14}CO_2$. In using such data we can take advantage of the longer record of the ^{14}C from nuclear weapons testing than was available for earlier model calibration studies such as that of Broecker et al. (1980). The uncertainty analysis considers the degree of agreement between the model and globally representative data. It is also relevant to consider any additional information concerning the atmospheric carbon budget that can be derived from the spatial distribution of CO_2.

The outline of the remainder of this report is as follows. Section 2 gives a brief description of the model, emphasising the extensions to the original box-diffusion model of Oeschger et al. (1975). Section 3 describes the strategy behind the choice of model runs presented here. Section 4 describes a Bayesian calibration of the model using the techniques described by Enting (1985a), Enting and Pearman (1983, 1986, 1987). Section 5.1 presents the results for our 'BASE' case

where the model is intended to be equivalent to that used for the IPCC (1990) report subject only to the changes required to give a consistent treatment of the terrestrial biota. Section 5.2 presents results based on a more extensive recalibration that tunes the oceanic CO_2 uptake. As mentioned above, the Bayesian calibration can provide an estimate of the extent to which the projections of the model are constrained by observational data. This is discussed further in Section 5.3. Section 5.4 presents results based on a range of alternative estimates of the past CO_2 flux from deforestation and other land-use changes. Section 6 reviews the overall implications of carbon budget uncertainty for the projections of CO_2. Section 7 gives a brief discussion of some aspects of the modelling study that are not directly related to the scenario calculations. For completeness, appendix A gives an abbreviated description of the assumptions and considerations underlying each of the scenarios used. Appendix B gives the sets of net carbon flux from land-use change that we use for the period prior to 1990. The data and the account of recent revisions (contributed by R.A. Houghton) are included here since the estimates are subject to continual refinement and specific cases have not always been readily available.

2. The Model

2.1 General

The model that we use is an extension of the box-diffusion model introduced by Oeschger et al. (1975). The characteristic feature of the model is its representation of the ocean: a surface mixed layer of fixed depth overlies a horizontally uniform deep ocean with vertical diffusive mixing. This mixing is parameterised by an eddy-diffusion coefficient, K. We have extended the original model of Oeschger et al. in a number of ways, some of which have previously been introduced in other studies (e.g. Siegenthaler and Oeschger, 1987). The main differences between the present model and the original 1975 version are:

1. We explicitly consider the three isotopes ^{12}C, ^{13}C and ^{14}C. In particular the inputs of ^{14}C are specified.
2. We use an explicit reservoir representation of the terrestrial biota as done by Siegenthaler and Oeschger (1987).
3. We introduce separate reservoirs for the stratosphere and troposphere; this allows a more realistic description of the ^{14}C inputs from nuclear weapons testing.
4. In the ocean, we include an explicit detrital transport with a fixed flux. This acts to establish a vertical concentration gradient for carbon and also acts to transport the additional ^{14}C from nuclear weapons testing in a manner that has no analogue for anthropogenic total carbon. Uptake of anthropogenic CO_2 by detrital transport can only occur if the detrital flux increases.
5. We use a non-linear form for the relation between CO_2 partial pressure and total inorganic carbon content in the mixed layer. This is of little importance for past centuries but will become progressively more important as atmospheric concentrations continue to rise.

k	Parameter, x_k	Units	1990	BASE	FITTED	q_k	w_k
1	Eddy diffusion	m^2y^{-1}	5364.5	5364.5	6245.2	5364	2000
2	Atmos. turnover	y	8.88	8.88	8.578	12	4
3	Buffer (at c_0)	—	9.36	9.36	9.36	9.36	n.a.
4	$c(0)_{\text{mixed}}(\text{ref})$	mol m^{-3}	2.089	2.089	2.089	2.089	n.a.
5	Carbonate pump	Gt C y^{-1}	( )	2.5	2.798	4	3
6	Initial CO_2	ppmv	*280	285.28	285.30	285	20
7	Stratospheric turnover	y	4	4	4	4	n.a.
8	Initial δ^{13}C	‰	( )	-6.4047	-6.4102	-6.5	0.2
9	$\Delta\delta^{13}$C $CaCO_3$ detritus	‰	( )	0	0	0	n.a.
10	Cosmic ray ^{14}C	'kg' y^{-1}	( )	5.0909	5.1549	6	2
11	Young biota	Gt	( )	140	140	140	n.a.
12	Old biota	Gt	( )	1400	1400	1400	n.a.
13	NPP	Gt C y^{-1}	( )	100	100	100	n.a.
14	T.over time of old biota	y	( )	60	60	60	n.a.
15	Future f.f. growth rate	% y^{-1}	n.a.	n.a.	n.a.	n.a.	n.a.
16	^{14}C from bombs[1]	'kg'/Mt	( )	2.7275	2.7929	2.75	0.30
17	Organic detrital pump	Gt C y^{-1}	( )	3	3.749	4	3
18	$\Delta\delta^{13}$C org. detritus	‰	( )	-24	-24	-24	n.a.
	Corrections to x_3						
19	Linear	—	59.56	59.56	59.56	59.56	n.a.
20	Quadratic	—	0	0	0	0	n.a.
21	Cubic	—	4558	4558	4558	4558	n.a.
	Enhanced growth						
22	Limit, G_∞	—	n.a.	2.4	2.4	2.4	n.a.
23	Fraction of biota	—	0	0.9692	0.9178	0.7	0.3

Table 1: Model parameters, x_k, their prior estimates, q_k, with corresponding uncertainties, w_k. The 1990 column gives the values used for the IPCC (1990) report. Brackets in the 1990 column denote parameters that did not affect the projections of CO_2. The '*' denotes the initial CO_2 concentration specified by the inversion of the ice-core data. The BASE and FITTED columns give the values used for, or fitted by, the present reference and extended cases, using the Bayesian calibration techniques. The n.a. entries denote 'not applicable'.

Further details of the processes are given in section 4.2 where the various model parameters are listed. The representation of the biota is described in section 2.3. Those parameters of the model whose uncertainties we judge to significantly affect the model predictions, are positioned in a parameter vector, **x**. There are 23 parameters so positioned $(x_1, \ldots, x_{23})$ and these are presented in Table 1. The model structure enables the elements of **x** to be readily tuned.

[1]Note in electronic edition: The 'kg' for parameter 16 refers to kg ^{14}C scaled by 12/14 as described in Section 4.2, giving 1 'kg' $= 10^{26}$ atoms ^{14}C.

The model works with the total amounts of carbon, ^{13}C and ^{14}C in a set of reservoirs that are taken as well-mixed. The isotopic data are included to aid in the model calibration. ^{13}C data are important in constraining the regional budgets derived from transport model fits to the observed spatial gradients, (Keeling et al., 1989b). Recently, Quay et al. (1992) have used ocean ^{13}C data to give a preliminary constraint on net ocean carbon uptake. However ^{13}C has little role to play in the global modelling calculations; Enting and Pearman (1986, 1987) showed that long-term rates of change of atmospheric ^{13}C provide essentially no new constraint. While there have been suggestions that deconvolutions of ^{13}C:^{12}C data from tree-rings would provide additional constraints (Peng et al., 1983), the work of Francey and Farquhar (1982) indicated that it is difficult to separate the effects of atmospheric changes from physiological influences on the isotopic composition. It should be possible to constrain the carbon cycle using ^{13}C:^{12}C of CO_2 from bubbles in polar ice, but it would require greater precision than that obtained by Friedli et al. (1986) in order to significantly constrain the model parameters. This is discussed further in section 7.2. Section 7.3 discusses the model results for oceanic $\delta^{13}C$ in terms of the recent study by Quay et al. (1992). Section 7.4 gives further discussion of our use of ^{14}C uptake in the oceans as a constraint on the model.

2.2 Forcing functions

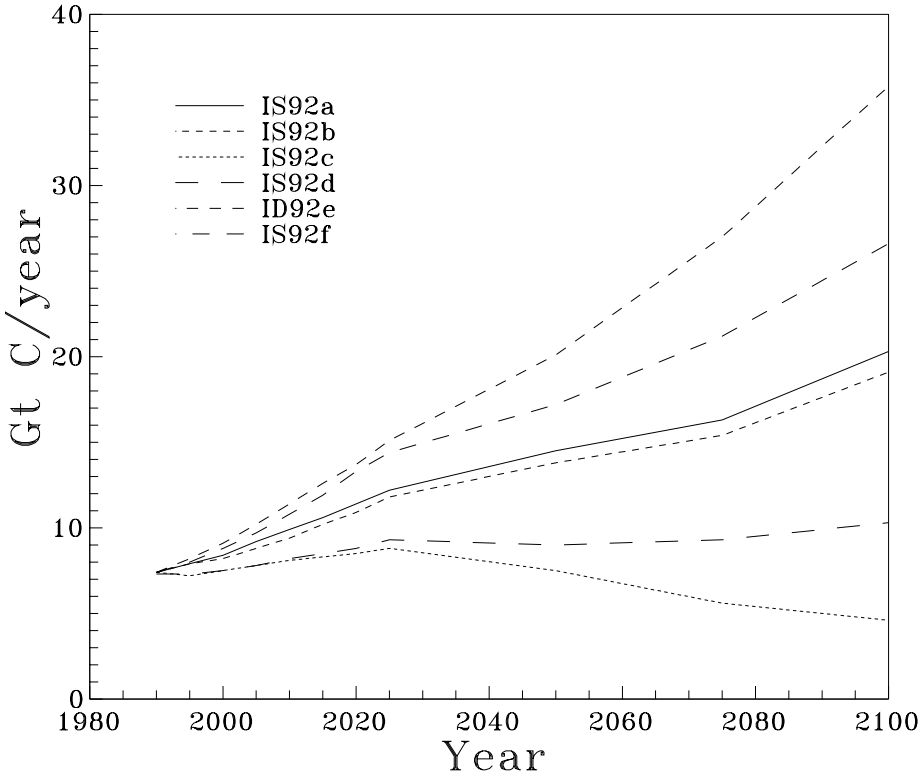

Figure 1: The 6 release scenarios presented in the IPCC (1992) report. Except for scenario IS92d, each case has a component of 1.3 Gt C y^{-1} from deforestation in 1990 — see Figure 2.

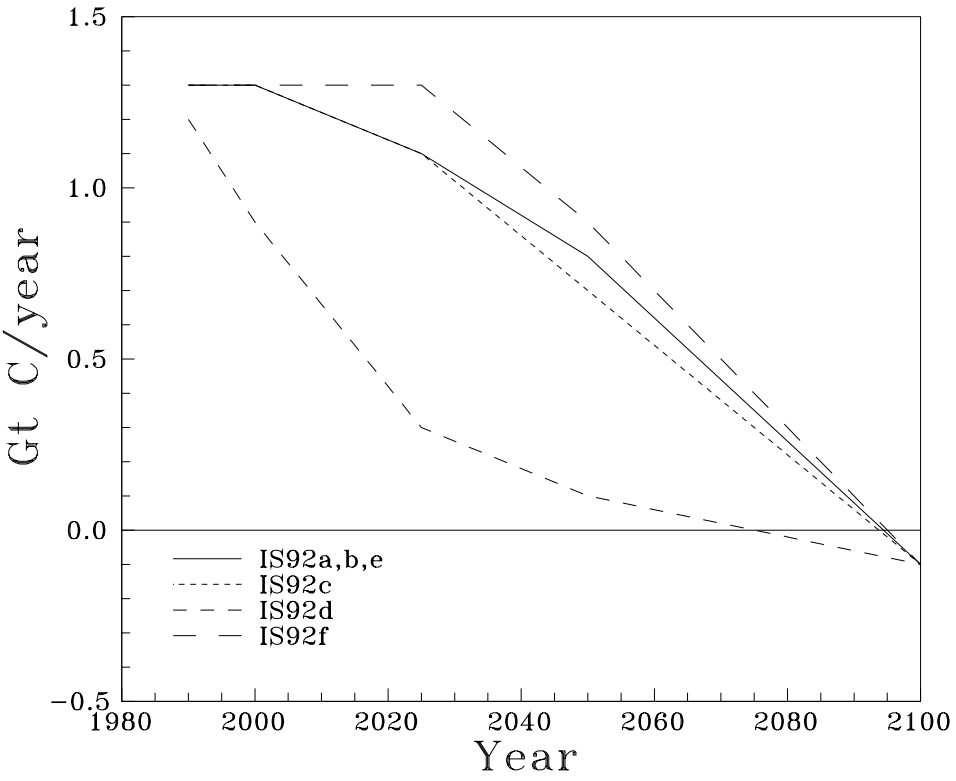

Figure 2: The 'deforestation' components of the IPCC release scenarios. For the period 1990 to 1995 we use a linear interpolation between these scenarios and the 1990 value of the past release estimates.

The equations that define the behaviour of the model involve a number of numerical parameters (see Table 1 and section 4.2). The values of these parameters define a pre-industrial equilibrium that is assumed to apply prior to 1800. (In running the model in this way, we have to consider the possibility (see Enting, 1992a) that the observations for 1800 do not actually reflect such an equilibrium). For the time evolution after 1800, the model requires the specification of a number of functions of time, representing 'forcing functions'. These are:

1. *Fossil carbon.* The fossil carbon release for the past is taken from CDIAC (1990). This is based on the work of Keeling (1973) for releases prior to 1950 and the work of Rotty (1987) and more recently Marland et al. (1989), Marland and Boden (1991). The future releases are prescribed by the IPCC (1992) scenarios as described in section 3.1. The IPCC scenarios are specified as total releases (shown in Figure 1) and a deforestation component (shown in Figure 2). The fossil component that we use is the difference between the two.

   An additional time function that is required by the model is for the ^{13}C:^{12}C ratio of the fossil carbon releases. For this we follow Enting and Pearman (1983, 1987) and use a piecewise linear approximation to the data of Tans (1981) (see Figure 3 of Enting and Pearman, 1987). Fossil carbon is devoid of ^{14}C due to its long isolation from the atmosphere.

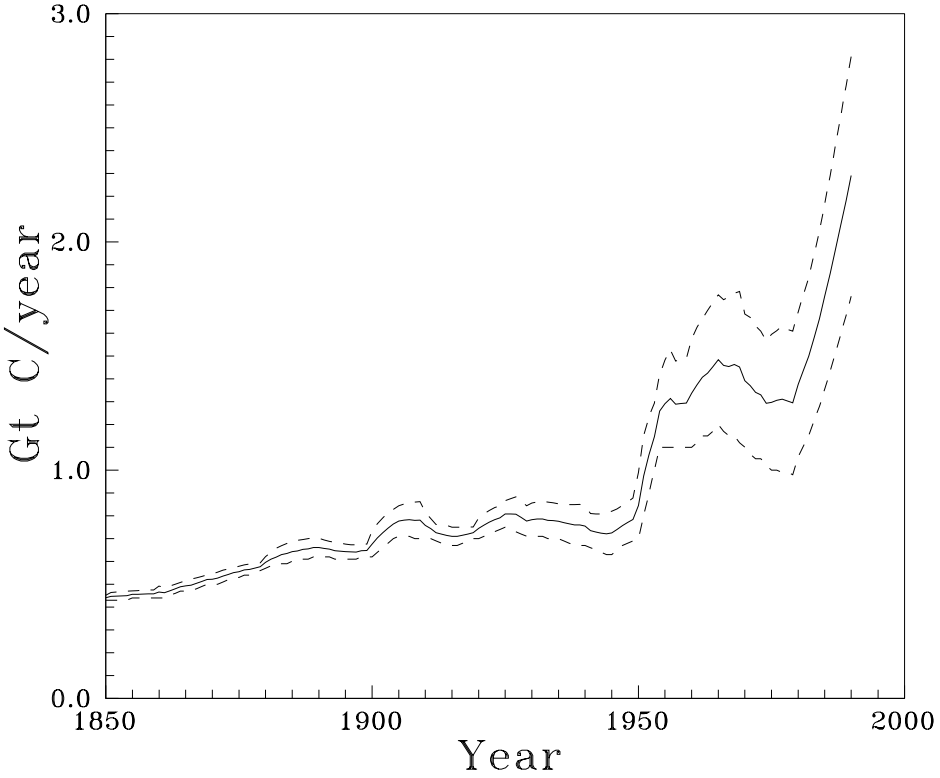

Figure 3: The 'land-use change' components used for the releases prior to 1990. The BASE and FITTED cases used the 'average' data set.

2. *Carbon from land-use changes.* The most comprehensive studies of carbon from past land-use change have been those of R. Houghton and co-workers. The primary reference is Houghton et al. (1983). These estimates have been refined and extended (Houghton et al. 1987; Houghton 1991, 1993, 1995; see also appendix B). The IPCC (1992) report presents scenarios of future deforestation as described in section 3.1 and shown in Figure 2. The estimates of past net releases associated with land-use changes are shown in Figure 3.

3. ^{14}C *from cosmic rays.* The rate of ^{14}C production by cosmic rays is taken as unvarying in time. Its actual value is tuned to match ^{14}C data from the time prior to nuclear weapons testing. The model structure provides the possibility of varying ^{14}C production rates, but this is mainly of relevance to longer-term studies concerned with ^{14}C-dating.

4. ^{14}C *from nuclear weapons tests.* The ^{14}C from nuclear weapons testing is specified by relating production to estimated energy yields. The data set used is given by Enting (1982) (or see Figure 4 of Enting and Pearman, 1987). An important reason for specifying the variation of the source with time rather than imposing a specified atmospheric history for the ^{14}C levels is that we can use the decrease in the period after the cessation of testing to check that the model gives the observed rate of decrease once the source goes to zero. (The ^{14}C release from nuclear reactors is small in comparison and is neglected; see Lassey et al., 1990). Because most of the ^{14}C produced by nuclear weapons testing was injected

directly into the stratosphere, it is appropriate for the model to have separate stratospheric and tropospheric reservoirs to reflect the relatively slow exchange between them.

5. CO_2 *history.* The observed history of changes in atmospheric CO_2 since 1800 is *not* used to force the model in the runs presented here. The calculations performed for the IPCC (1990) report forced the atmospheric CO_2 concentration to track a fit to the CO_2 record defined by the combination of ice-core data and direct measurements for the period 1800 to 1990. The model then deduced the biomass changes that were needed to balance the budget. As noted above such an 'inverse modelling' approach makes it difficult to ensure a consistent treatment of the terrestrial biota and so all results presented in this report are from 'forward modelling'.

2.3 The terrestrial biota

The terrestrial biota is represented in terms of two reservoirs denoted 'short-lived' and 'long-lived', terms which refer to the residence times (some of the 'long-lived' component represents dead organic carbon). The carbon contents of these reservoirs are denoted $N_{\rm S}$ and $N_{\rm L}$.

The rates of change of carbon contents of these reservoirs are given by:

$$\dot{N}_{\rm S} = P(t) - \lambda_1 N_{\rm S} - \lambda_2 N_{\rm S} \tag{2.1}$$

$$\dot{N}_{\rm L} = \lambda_2 N_{\rm S} - \lambda_{\rm L} N_{\rm L} - D(t) \tag{2.2}$$

and where $P(t)$ represents the net primary production (NPP), $D(t)$ is the rate of carbon release associated with land-use change and $\lambda_{\rm L}$, λ_1 and λ_2 are rate constants (or inverse turnover times) defining the fluxes from the biotic reservoirs. As discussed below, $D(t)$ represents a 'gross' flux rather than a net flux associated with land-use change.

The terrestrial reservoirs are subject to the initial conditions:

$$N_{\rm S}(t_0) = x_{11} = \ 140 \text{ Gt C} \tag{2.3a}$$

$$N_{\rm L}(t_0) = x_{12} = 1400 \text{ Gt C} \tag{2.3b}$$

The natural turnover rate of the long-lived reservoir and the pre-industrial primary production, $P(t_0)$ are expressed in terms of the model parameters by:

$$\lambda_{\rm L}^{-1} = x_{14} = 60 \text{ years} \tag{2.4a}$$

$$P(t_0) = x_{13} = 100 \text{ Gt C y}^{-1} \tag{2.4b}$$

Carbon loss from the short-lived reservoir is then defined by the requirement of pre-industrial equilibrium so that:

$$\lambda_2^{-1} = \lambda_{\rm L}^{-1} N_{\rm S}(t_0)/N_{\rm L}(t_0) = 6 \text{ years} \tag{2.4c}$$

and

$$\lambda_1^{-1} = (P(t_0)/N_{\rm S}(t_0) - \lambda_2)^{-1} = 1.826 \text{ years} \tag{2.4d}$$

The changes in the terrestrial biota give a carbon flux to the atmosphere of

$$F_{\text{Biota} \rightarrow \text{Atmosphere}} = \lambda_1 N_{\text{S}} + \lambda_{\text{L}} N_{\text{L}} + D(t) \tag{2.5}$$

In equilibrium, with $D(t) = 0$, this flux balances the NPP.

The isotopic composition of each inter-reservoir flux is taken as that of the source reservoir, except for the primary production, $P(t)$, which is subject to isotopic fractionation during photosynthesis [1]. The 'deforestation', $D(t)$, is presumed to augment the natural decay so that the 'long-lived' reservoir is always the source of the flux $D(t) + \lambda_{\text{L}} N_{\text{L}}$, even if $D(t) < 0$.

In the model, the natural state of the long-lived component of the biota represents a balance between the input and output given by

$$\lambda_2 N_{\text{S}} = \lambda_{\text{L}} N_{\text{L}}$$

If there is a deforestation that leads to a reduction of N_{L} then the 'natural' loss rate will be reduced and the biota will tend to return to its equilibrium. The estimates from Houghton of the carbon releases due to land-use change are intended to represent the *net* result of both release and recovery. Denoting such net releases as $B(t)$, we need to define

$$D(t) = B(t) + \lambda_{\text{L}} \int_{t_0}^{t} B(t')\, dt' \tag{2.6}$$

so that the gross flux $D(t)$ has the net effect of changing N_{L} at the rate $B(t)$. Equation (2.6) must be regarded as a mathematical transformation to produce a function $D(t)$ which gives the correct net flux, $B(t)$. Because of the simple structure of the model, the $D(t)$ calculated in this way will in general not correspond to actual gross fluxes arising from land-use change. Specifically, the reduction in the loss $\lambda_{\text{L}} N_{\text{L}}$ once $D(t)$ has reduced N_{L} will in part correspond to regrowth, but the size of the effect is likely to be larger than is realistic because λ_{L} is chosen to represent the time-scales of natural turnover rather than the time-scales of ecosystem succession or societal changes.

The possible enhancement of biotic growth in response to elevated levels of atmospheric CO_2 (and possibly other nutrients) is the least certain component of the atmospheric carbon budget. Global-scale estimates are derived primarily from modelling studies such as those of Kohlmaier et al. (1987), Gifford (1993) and Polglase and Wang (1992).

The effect of CO_2-enhanced growth is expressed as a multiple of the 'unfertilised' primary production as

$$P(t) = P(t_0)(1 + x_{23}(G(C) - 1)) \tag{2.7}$$

where $G(C)$ represents the relative enhancement in growth for an atmospheric CO_2 concentration C and x_{23} specifies the proportion of the NPP to which this enhancement applies. The value of x_{23} is obtained by fitting the data. This parameter should in principle lie between 1 and zero but the limit of 1 pre-supposes that the primary production, x_{13} is correct. Since the model

[1] Note added in electronic edition: A fractionation factor of 0.982 is used.

is insensitive to the choice of the net primary production, we do not try to fit it to the data and do not regard values of x_{23} that are slightly above 1 as being unacceptable.

We represent the CO_2-enhanced growth in the hyperbolic form described by Allen et al. (1987).

$$G(C) = G_\infty \frac{C - C_c}{C + b} \tag{2.8}$$

where G_∞ is the limiting growth factor, C_c is the compensation concentration below which photosynthesis ceases, taken to be 80 ppmv after Allen et al. (1987). The condition $b = (G_\infty - 1)C_0 - G_\infty C_c$ ensures that $G(C_0) = 1$ at the initial concentration $C_0 = x_6$. We use $G_\infty = x_{22} = 2.4$, which is at the higher end of the values discussed by Allen et al. (1987). Smaller values of x_{22} required x_{23} rather greater than 1 to achieve a balanced carbon budget.

Allen et al. (1987) have also expressed their formalism in terms of the so-called β-factor that has been traditionally used in carbon cycle studies. However Enting (1995) suggested that for talking about carbon budgets it would be preferable to have a measure of carbon *storage* rather than uptake. He proposed using the 'biota-atmosphere growth ratio' as such a measure, noting that for linearised responses and exponential forcing, the ratio would be a constant and would also be independent of the characteristics of the oceanic CO_2 uptake. Some of the model results in section 5 are expressed in such terms.

3. Model Runs

3.1 Scenarios

The IPCC (1992) report presents 6 scenarios for CO_2 emissions for the period 1990–2100. The total CO_2 emissions for each scenario are shown in Figure 1. The corresponding contributions from land-use changes are shown in Figure 2. Each of these 'deforestation' components has a 1990 release of 1.3 Gt C y^{-1}, except for scenario IS92d which has the slightly lower value of 1.2 Gt C y^{-1} for 1990. These are significantly lower than either of the 'high' and 'low' releases estimated for 1990 by Houghton (1991, 1993, 1995) (see Figure 3 and appendix B contributed by R.A. Houghton).

The emissions in the IPCC scenarios are specified at 5 year intervals from 1990 to 2025 and at 25 year intervals thereafter, i.e. at 11 time points. The scenarios specify total release rates at these times, and the contributions from deforestation less frequently. We use linear interpolation to determine the separate 'fossil' and 'deforestation' sources at the 11 time points. The model then adopts linear interpolation to determine release rates at intermediate time steps.

3.2 Cases considered

Base case: Our first set of projections uses the model in a form close to that used in previous calculations with the scenarios from the IPCC (1990) report, except that the procedure is modified to produce a balanced carbon budget with consistent treatment of the biota. The main aspects of the calculations are:

1. It is a forward calculation throughout the period 1800–2100, rather than being an inverse calculation (with the concentration tracking the ice-core data) for the period 1800–1990. Using a forward calculation means that fitting the observed rate of change of atmospheric CO_2 is no longer automatic, as it is in an an inverse calculation, but a forward calcultion can ensure consistent treatment of the biota throughout the period.

2. The biomass change is specified as a combination of a 'deforestation' term and a CO_2-enhanced growth ('fertilisation'). The deforestation term to 1990 is taken from the average of the 'low-release' and 'high-release' estimates from Houghton (see appendix B). In order to merge the scenarios' 1.3 Gt C y^{-1} (or 1.2 Gt C y^{-1}) release with the much larger value for 1990 in the Houghton time series, we apply a linear decrease from the Houghton estimate for 1990 to the scenario value for 1995. This is an *ad hoc* way of dealing with a discrepancy, but the issues involved are extremely complex. Our approach is to regard the IPCC scenarios as possible targets that cannot be achieved instantaneously and of course 1990 has passed and there is little definite evidence of a sudden decrease in deforestation rate. Since the IPCC (1992) scenarios (except for IS92d) assume that deforestation continues to the limit of available forest, it is clear that higher deforestation rates could only be sustained for a short time and so our rapid 'cross-over' seems to be an acceptable approximation to plausible future deforestation patterns.

3. The fertilisation fraction (x_{23}) and the initial CO_2 concentration (x_6) are adjusted to give the best fit to the 20th century CO_2 record (i.e. ice-core data plus direct measurement), recognising that the work of Enting (1992a) shows that it will be impossible to fit the whole of the ice-core record since 1800. Enting (1992a) concluded that the early increase in atmospheric CO_2 reflected a recovery from a temporary decline in concentration, possibly associated with the little ice-age, but in any case reflecting some 'natural' process showing non-stationary behaviour and thus lying outside the range of validity of the present model.

4. All other model parameters (and forcing functions) affecting the uptake of total carbon remain the same as in the previous calculations. In particular the two most important parameters, the eddy diffusion coefficient and the air-sea gas exchange coefficient, are taken from the work of Broecker et al. (1980). As emphasised by Enting (1991), the values chosen are *not* based on carbon cycle data so that the prior values should be independent of other parameters, notably the size of the detrital transport. The eddy diffusion coefficient is taken as 5364.5 m^2y^{-1} (on the basis of tritium data) and the air-sea gas exchange rate is expressed in terms of an atmospheric turnover time of 8.88 years on the basis of radon data.

5. The parameters affecting the isotopic distributions (x_8, x_{10} and x_{16}) are adjusted so that the model is consistent with isotopic data. To a first approximation, the ^{14}C parameters x_{10} and x_{16} define the amplitude of the ^{14}C signal; the time characteristics of ^{14}C changes provide a check on the internal consistency of the model. Alternatively, in the FITTED case described below, the time characteristics of ^{14}C provide the information to constrain the oceanic uptake.

6. Given these conditions, all 6 scenarios are considered.

Extended calibration: In addition to fitting the 5 parameters x_6, x_{23}, x_8, x_{10} and x_{16} as in the base case, the FITTED case also tunes x_1, x_2, x_5 and x_{17}. Varying x_1 and x_2 allows the oceanic CO_2 uptake to be tuned. The detrital flux parameters x_5 and x_{17}, the two 'pump strengths', are adjusted so that the CO_2 and ^{14}C uptake rates can, to some extent, vary independently as noted in section 2.1. A semi-analytic investigation of this is given by Enting (1990).

Uncertainty analysis: The BASE and FITTED cases have the parameters estimated using the calibration procedure described in section 4 below. As well as producing a set of 'best-fit' parameters, the calibration procedure can also produce estimates of the range of uncertainty in quantities calculated by the model. We use this formalism (described by Enting and Pearman, 1983, 1986, 1987) to estimate the range of uncertainty in the projected CO_2 concentrations for the year 2100, by allowing variations in the same 9 parameters as in the FITTED case.

Modified atmospheric budget: A further set of calculations were performed to explore the implications of the uncertainty in the atmospheric carbon budget. Firstly we considered the uncertainty in the 'deforestation' source. This was done by using the 'high' and 'low' releases from Houghton (see appendix B) in place of the average used in the BASE and FITTED cases. For each release history, the model was re-calibrated fitting the same 9 parameters as in the FITTED case. The best-fit calibrations for these cases each had approximately the same oceanic uptake — to a large extent the changed release was accomodated by changes in the fertilisation. Secondly, we explored the scope for acceptable variation in oceanic uptake. Because the ocean parameterisation does provide a single parameter for specifying ocean uptake, we forced such variation by considering a range of specified terrestrial contributions. We performed a sequence of calibrations, each with the fertilisation parameter x_{23} fixed at a specified value in the range 0.6 to 1.3, and with a common deforestation history.

4. Calibration

4.1 Techniques

Since the box-diffusion model is highly parameterised, it needs to have the parameters calibrated before it can be used to make projections of future CO_2 concentrations. This is done by ensuring that the model reproduces observable aspects of the carbon cycle, particularly the distributions of ^{14}C from natural cosmic-ray sources and from nuclear weapons tests after 1945 and the observed changes in atmospheric CO_2.

The original calibration method used by Oeschger et al. (1975) was determined by mathematical convenience — the simple analytic structure of the solutions made it possible to find many cases in which parameters were uniquely indentified with particular combinations of data.

For a more general approach, the most obvious technique is to use a least-squares fit to the

available carbon cycle data, adjusting the model parameters to minimise the sum of squares of differences between model results and observations. However the work of Enting and Pearman (1982, 1983) shows that this procedure is ill-conditioned and so it is subject to instability. They proposed (Enting and Pearman, 1983, 1986, 1987) a Bayesian approach of minimising the sum of squares of deviations from observations plus the sum of squares of deviations of the parameters from independent prior estimates.

We define

$$\Theta = \sum_j (y_j(\mathbf{x}) - m_j)^2 / v_j^2 + \gamma \sum_k (x_k - q_k)^2 / w_k^2 \qquad (4.1a)$$

where **x** denotes the parameter vector, $(x_1 \ldots x_{23})$, q_k denotes the prior estimate of parameter k, w_k denotes the standard deviation of this estimate, $y_j(\mathbf{x})$ denotes the model result for the jth data item, expressed as a function of the model parameters, m_j denotes the corresponding observed value and v_j denotes its standard deviation of the observed value. Table 1 lists the parameters and the values of the q_k and w_k. Tables 2 and 3 list the observed data and the m_j and v_j values. Tarantola (1987) gives an extensive discussion of ill-conditioned inversion problems, taking the Bayesian approach as fundamental.

Table 1 gives the full list of parameters required as input to the model. Only a subset, A, of the parameters are adjusted in this work and so the definition of Θ is replaced by

$$\Theta = \sum_j (y_j(\mathbf{x}) - m_j)^2 / v_j^2 + \gamma \sum_{k \in A} (x_k - q_k)^2 / w_k^2 \qquad (4.1b)$$

The calibration produces a set of 'best-fit' parameters to be used in calculating the projected CO_2 concentrations.

Uncertainties in the calibration will be reflected in uncertainties in the projections. Enting and Pearman (1983, 1986, 1987) analysed this problem for an arbitrary quantity, Z, calculated by the model. The determination of the possible range of Z subject to some specified goodness-of-fit to the calibration data, is expressed as finding the extremes of Z subject to $|\Theta - \Theta_{\text{min}}| \leq c$ for some suitable c. This problem can be solved by introducing a Lagrange multiplier, α, and seeking the extrema of

$$\Theta^* = \Theta - \alpha Z \qquad (4.2)$$

In the applications below, we take Z to be the calculated CO_2 concentration for the year 2100.

The Bayesian calibration technique has previously been applied to the carbon cycle model of Pearman (1980) by Enting and Pearman (1983, 1986, 1987). An alternative technique of uncertainty analysis that has been used in carbon cycle modelling is the Monte Carlo approach (Gardner and Trabalka, 1985). Laurmann and Spreiter (1983) estimated the range of uncertainty in projected CO_2 levels on the basis of a series of sensitivity studies of carbon cycle models.

The minimisations are performed using the simplex algorithm of Nelder and Mead (1965). The implementation that we use is the pascal routine 'amoeba' given in Press et al. (1986). The simplex algorithm was chosen on the basis of experience that found it to be more stable than

several alternatives based on numerically-determined derivatives. However for the shallow minima that occur in ill-conditioned problems such as the present calibration problem, the simplex algorithm may perform relatively poorly at finding the precise location of the minimum. The objective function will be close to the true minimum value but the parameters may be noticably different from those specifying the true minimum. The consequences of this are:

- The parameters quoted for particular cases must be regarded as representative of a set that gives the level of agreement specified by the value of Θ_{min} rather than defining the precise location of the minimum.
- Consequently, the quoted parameter values for a set of related cases may show minor inconsistencies.
- In particular, sequences of parameter changes determined from smooth changes in one of the conditions may vary less smoothly than expected.

4.2 Parameters

In this report, systematic investigation is confined to 9 of the 23 parameters in Table 1. The choice of which parameters to investigate is based on our judgements concerning the uncertainty, combined with the results from Enting and Pearman (1983, 1986, 1987) who performed a more extensive study of the relative importance of parameters in carbon cycle models. The 9 parameters are those for which ranges of uncertainty w_k are quoted in the final column of Table 1. The column headed '1990' lists the values used in the calculations contributed for the IPCC (1990) report. In particular, Figures 1.7 and 1.8 of the IPCC (1990) report show results for the 'science scenarios' from the present model (run in inverse mode to 1990) using the parameters from the '1990' column of Table 1, or from some model with indistinguishable behaviour. The attribution, in the IPCC (1990) report, of those results to the model of Enting and Pearman (1987) is incorrect. The results for the 'policy scenarios' reported in the IPCC (1990) report are based on a model whose behaviour differs only slightly from the present model.

The empty brackets in the column headed '1990' indicate those parameters that do not affect CO_2 projections: they concern instead the isotopic distribution or define the steady-state characteristics of the marine and terrestrial biota. This helps explain the origin of the ill-conditioning of the calibration process: in order to use isotopic data for model calibration, a three-fold increase in the number of model parameters is required.

The column of Table 1 headed 'BASE' shows the parameter values used in our reference case. Except for the 5 parameters explicitly tuned (x_6, x_{23}, x_8, x_{10} and x_{16}) together with parameter x_{22} which needs to be specified once the model includes a CO_2-enhanced growth, the remaining 17 are taken from the '1990' case. (Note that x_{15} represents an unused 'default' extrapolation of fossil fuel growth and is not relevant to any of the calculations described here). The single isotopic parameter (the initial atmospheric δ^{13}C, x_8), is constrained by one contemporary atmospheric value, ^{13}C plays no actual role in the calibration and is included only for completeness

and as a basis for the discussion of sections 7.2 and 7.3.

The column of Table 1 headed 'FITTED' records the results of the more comprehensive calibration.

In assigning prior estimates (q_k) and corresponding ranges of uncertainties (w_k) to the parameters, we draw heavily on the work of Enting and Pearman (1983, 1986, 1987) who applied the Bayesian calibration approach to the similar carbon cycle model of Pearman (1980).

We summarise below our choices for the 22 parameters (x_{15} being irrelevant) and those of the 'prior values', q_k, and ranges, w_k, for those that we adjust.

1: *Diffusion coefficient.* For the 'BASE' case we adopt the value 5364.5 m^2 y^{-1} as proposed by Broecker et al. (1980) on the basis of tritium distributions. For the prior estimate and range for the 'FITTED' case we use a rounded value and broad range, 5364 ± 2000 m^2 y^{-1}, so that the value of K is determined primarily by the carbon cycle data.

2: *Air-sea gas-exchange rate.* This is expressed as a turnover time for the atmospheric CO_2 with respect to gas exchange into the ocean mixed layer. The BASE case adopts 8.88 year corresponding to the value derived from radon evasion by Broecker et al. (1980). The fact that our FITTED case leads to a similar value suggests that it is generally consistent with carbon cycle data. However the analysis of gas exchange by Liss and Merlivat (1986) suggests gas exchange rates of about half those implied by carbon cycle data. Therefore in the FITTED case, we commenced with a prior value of 12 ± 4 yr to accomodate such smaller gas exchange rates.

3, 4, 19, 20, 21: *Buffer factor.* The buffer factor ξ describes the variation of $p_{\mathrm{CO}2}$ as a function of dissolved inorganic carbon concentration. The formalism follows Bacastow (1981). The $p_{\mathrm{CO}2}$ of the mixed layer is given as

$$P = P_0[1 + y\xi(y)]$$

with a reference partial pressure, $P_0 = 290$ ppmv and $y = (q - q_0)/q_0$ with q being the dissolved inorganic carbon concentration in the mixed layer and $q_0 = 2.089$ moles m^{-3}. The buffer factor ξ is expressed as:

$$\xi(y) = x_3 + x_{19}y + x_{20}y^2 + x_{21}y^3$$

We use the values from Bacastow (1981) of

$$\xi(y) = 9.36 + 59.56y + 0y^2 + 4558y^3$$

The reference concentration, q_0 is set as parameter x_4 to provide the capability to vary this quantity. In the present study, we do not explore the range of uncertainty in the relation between concentration and $p_{\mathrm{CO}2}$.

5, 9, 17, 18: *Detritus.* The model represents two types of detrital flux, denoted 'organic' and 'carbonate'. The model distinguishes these two types of detritus in terms of the depth

of re-mineralisation and the isotopic fractionation relative to the inorganic carbon in the surface water. The rate of re-mineralisation of the organic component decreases exponentially with depth (Martin et al., 1987); the carbonate component re-dissolves in equal proportions at all depths. Each detrital component is characterised by a fixed rate (in Gt C y^{-1}) of export of carbon from the surface (the 'pump strengths'), and a fractionation parameter giving the ^{13}C depletion (relative to the surface water) of the detrital flux. The chosen fractionations also specify the depletion of ^{14}C through the usual thermodynamic assumption on the dependence of fractionation upon isotopic mass.

The strengths of the pumps are subject to considerable uncertainty. It should be noted that most estimates are based in some way on model calculations. Therefore for our purposes we need to start with large uncertainties and estimate the pump strengths from the carbon cycle data, taking into account all the other parameter uncertainties. Recent estimates have been as large as 10 Gt C y^{-1} or more for the combined pump strength (e.g. Najjar et al., 1992; Sarmiento and Siegenthaler, 1992). However this has in part reflected the assumption of a large role for dissolved organic carbonate (DOC). Since the measurements that suggested large DOC concentrations have recently been questioned, we have chosen somewhat lower values and use 4 ± 3 Gt C y^{-1} for each pump strength.

Isotopic depletion upon detrital formation is taken as $0‰$ for the inorganic component and $-24‰$ for the organic component and are based on results from Rau et al. (1989, 1992). These rounded values are adequate for the studies presented here in which the marine biota are in a steady state but a more precise representation may be required for studies of changes in the ocean ^{13}C balance.

6: *Initial CO_2 concentration.* The uncertainties concerning the pre-industrial conditions have led us to take the prior value of 285 ppmv (corresponding to ice-core data from the middle of last century) and assign a large uncertainty of ± 20 ppmv, so that x_6 is determined mainly by the fit to the later CO_2 data.

7: *Stratospheric turnover time.* Empirical determination of an appropriate stratospheric turnover time is subject to considerable difficulty because the concept, as used here, is defined relative to a well-mixed stratosphere. The approach we have used here is to consider the tropospheric response to input of a long-lived tracer and relate the initial loss from the troposphere to a stratosphere-troposphere exchange. Enting (1985b) parameterised the response to CFC-11 inputs in a two-dimensional atmospheric model in a form that translates to a stratospheric turnover time of a little over 3 years. For the present study, we use 4 years.

8: *Initial atmospheric $\delta^{13}C$.* The ice-core data of Friedli et al. (1986) suggest $-6.5 \pm 0.2\,‰$. The ^{13}C specification is included for completeness but it effectively plays no part in the calibration. The possible applications of ^{13}C data are discussed in section 7.

10: *Production of ^{14}C from cosmic rays.* The units of ^{14}C used in the model are kilograms scaled by $\frac{12}{14}$ — the scaling is introduced since the model works with masses for total carbon but molar quantities for isotopic ratios. (A factor of 10^{12} is implied by working in Mt for the two stable isotopes and 'kg' for ^{14}C). The ^{14}C production rate from cosmic rays was calculated (as a function of time) by O'Brien (1979) as varying over a range 1.6 to 1.9 atoms $cm^{-2}s^{-1}$. From this range, Enting and Pearman (1983, 1987) used a mean of

1.4 $\times 10^{-5}$ mol s^{-1} for the whole earth. In terms of the scaled kilograms, this converts to 5.6 'kg' ^{14}C per year. We use only the most significant figure and apply a range of $\pm$33% (c.f. $\pm$25% used by Enting and Pearman) to give: 6.0 ± 2.0 'kg' ^{14}C per year.

11, 12, 13, 14: *Terrestrial biota.* As described in section 2.3, the 'natural' state of the terrestrial biota is described in terms of 4 independent parameters: an initial size and a carbon exchange rate for each of the two reservoirs used to represent the terrestrial biota. The sizes, 140 GtC and 1400 GtC, are taken directly from Enting and Pearman (1983, 1987) who considered a range of biomass estimates. Similarly the fluxes, expressed as an NPP of 100 Gt C y^{-1} into the short-lived component and a turnover time of 60 years for the long-lived component are taken from Enting and Pearman (1983, 1987).

16: *Production of ^{14}C from weapons tests.* We use 2.75 ± 0.3 'kg' per megaton effective yield, where the mass units are scaled as described in connection with cosmic ray production of ^{14}C. Enting and Pearman (1983, 1987) used a prior value of 4.0 'kg' per Mt corresponding to the estimate 2.0×10^{26} atoms per megaton from Machta et al. (1963). However their calibration indicated a smaller value. The present value corresponds to 1.5×10^{26} atoms per megaton.

22, 23: CO_2*-enhanced growth.* As described in section 2.3, the enhanced growth is represented by a hyperbolic response to the atmospheric CO_2 concentration. The hyperbolic form is specified by the CO_2 compensation concentration (b in equation 2.8) which we take as 80 ppmv following Allen et al. (1987), and the limiting growth factor G_∞. Our model includes the capability of adjusting G_∞ by defining $G_\infty = x_{22}$. For the calculations presented here, we take the value $x_{22} = 2.4$, again following Allen et al. (1987). This enhancement is taken as applying to only a fraction of the net primary production; the proportion is specified by parameter x_{23} which is estimated by fitting the atmospheric CO_2 data. This proportion will differ from 1 for ecosystems that are not CO_2-limited and for those with C-4 photosynthesis dominant. Given the large uncertainties, we use a value of 0.7 ± 0.3 as our prior estimate, recognising that most estimates of the global carbon budget require a significant 'fertilisation' effect.

4.3 Carbon cycle data

As with the model parameters, our choice of the set of carbon cycle data to use in the calibration closely follows that of Enting and Pearman (1983, 1986, 1987). The main differences are the availability of ice-core data for CO_2 for the present analysis, the lack of a distinction between warm and cold oceans in the present box-diffusion model and the longer atmospheric ^{14}C record now available.

The various data sets that were used were:

Ice-core CO_2 concentration. The data are selected from Friedli et al. (1986), neglecting the earlier data because of our concern that 1800 may not represent a pre-industrial equilibrium. The data are assigned an uncertainty of ± 5.0 ppmv.

Direct measurements of atmospheric CO_2. The calibration data are taken as the annual averages at 3-year intervals, from Keeling et al. (1989a) and assigned an uncertainty of ± 1 ppmv. We make no attempt to incorporate an offset for the difference between the Antarctic and Hawaii. The spatial distributions presented by Keeling et al. (1989b) indicate that the interhemispheric gradient has largely arisen in the last few decades and that the gradient was small at the time (1953–1959) where we merge the direct data with the ice-core data (Keeling et al., 1989a). The CO_2 data are listed in Table 2 and plotted in Figure 4.

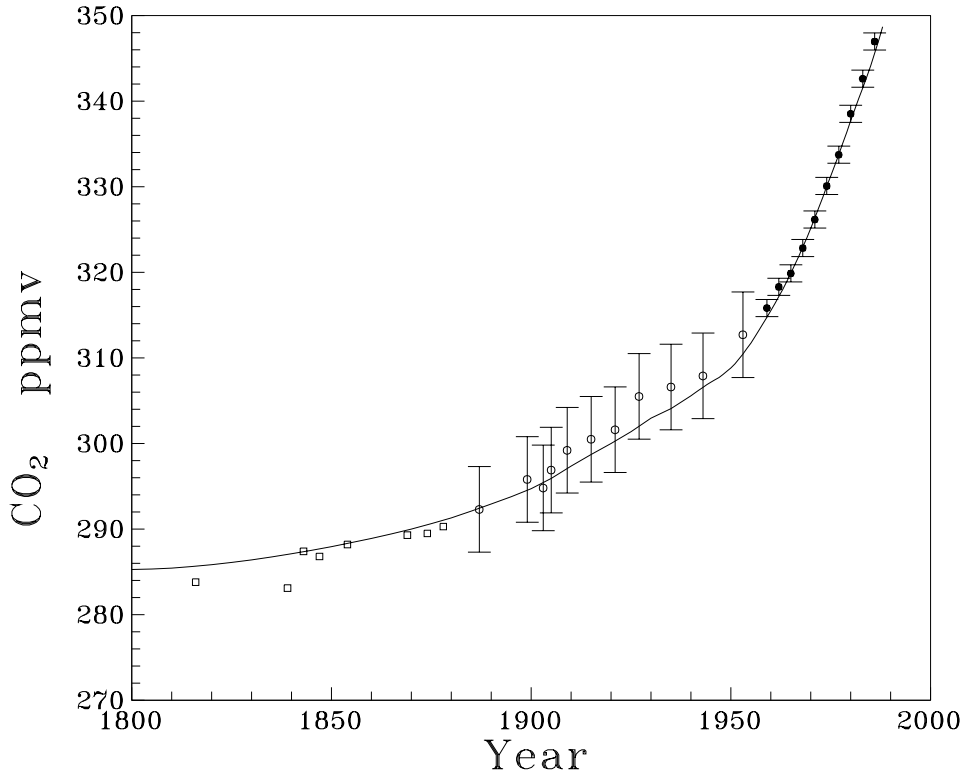

Figure 4: The atmospheric CO_2 levels for the BASE case of the model (solid line), compared to the data used in the calibration (shown with error bars). The filled circles are data from Keeling et al. (1989a). The open circles are from Friedli et al (1986). The open squares show data from Friedli et al. that were not used in the calibration.

Atmospheric ^{14}C. A comprehensive survey of atmospheric ^{14}C was presented by Nydal and Lövseth (1983). As discussed further in section 7.1 below, we only use data from the period after the nuclear testing. Figure 5 plots the ranges we use and for comparison shows two long time series for single sites. For the northern hemisphere we show the data for Vermunt from Levin et al. (1985) and for the southern hemisphere we show data for Wellington, New Zealand from Manning et al. (1990). We also show the short record from Cape Grim, Tasmania (Levin et al., 1990, 1991). The ranges we use are based on the spread of values reported by Nydal and Lövseth (1983). In particular the range decreases with time as the spatial variability within the atmosphere decreases.

Reservoir	Quantity	Units	Time	Value	s.d	Time	Value	s.d
Trop.	CO_2	ppmv	1887	292.3	5	1959	315.83	1
Trop.	CO_2	ppmv	1899	295.8	5	1962	318.30	1
Trop.	CO_2	ppmv	1903	294.8	5	1965	319.87	1
Trop.	CO_2	ppmv	1905	296.9	5	1968	322.83	1
Trop.	CO_2	ppmv	1909	299.2	5	1971	326.16	1
Trop.	CO_2	ppmv	1915	300.5	5	1974	330.08	1
Trop.	CO_2	ppmv	1921	301.6	5	1977	333.73	1
Trop.	CO_2	ppmv	1927	305.5	5	1980	338.52	1
Trop.	CO_2	ppmv	1935	306.6	5	1983	342.16	1
Trop.	CO_2	ppmv	1943	307.5	5	1986	346.96	1
Trop.	CO_2	ppmv	1953	312.7	5	—	—	—

Table 2: Atmospheric CO_2 data used in the calibration of the model. Note that the concentrations are annual means and so the times refer to the middle of the year, i.e. the last value refers to $t = 1986.5$ in the model.

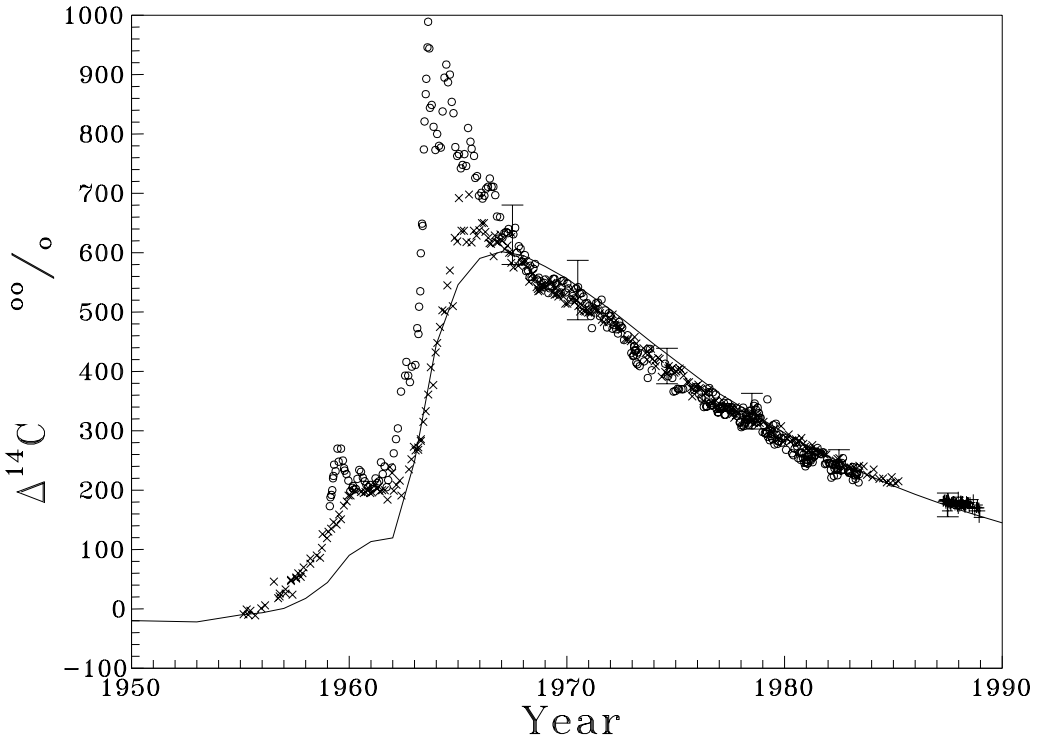

Figure 5: The atmospheric ^{14}C levels for the BASE case of the model, compared to the data used in the calibration. The solid line is the calculated value. The data used in the calibration is shown with error bars. The points show the original data from which these calibration values were derived. 'o' is northern hemisphere data from Vermunt (Levin et al., 1985), 'x' is New Zealand data (Manning et al., 1990), '+' is Cape Grim data.

Biotic ^{14}C. The biotic ^{14}C data are included to define the 'Suess effect', the decrease in atmospheric Δ^{14}C due to release into the atmosphere of fossil carbon which is free of ^{14}C. The data were from a tree-ring study by Lerman et al. (1970).

Ocean ^{14}C. The ocean ^{14}C datum for 1973 is a composite value based on data from the GEOSECS program (see for example, Broecker et al., 1985). The 1958 value is from early work by Broecker et al. (1960).

Deep ocean inorganic carbon. The vertical gradient of carbon concentration in the oceans is due to the detrital transport. We include the deep ocean value (from GEOSECS data) to constrain the detrital transport in the model. The surface concentration is essentially constrained by our formalism for relating concentrations to p_{CO2}.

The calibration data, other than those for atmospheric CO_2, are listed in Table 3.

One aspect of the data analysis that we have not explored here is an assessment of the relative importance of the various items of calibration data. Enting and Pearman (1986, Table 21.2) presented such an analysis, ranking their calibration data both for importance in defining the 'best-fit' and for constraining the range of variation in projected atmospheric CO_2 concentrations. Ranking the various items within the time series of atmospheric CO_2 and ^{14}C is of little significance. What was apparent however was the small importance of the 'Suess effect' data and the deep ocean carbon concentrations for Enting's and Pearman's work.

Reservoir	Quantity	Units	Time	Value	s.d
Trop.	Δ^{14}C	‰	1967	630	50
Trop.	Δ^{14}C	‰	1970	537	50
Trop.	Δ^{14}C	‰	1974	409	30
Trop.	Δ^{14}C	‰	1978	333	30
Trop.	Δ^{14}C	‰	1982	248	20
Trop.	Δ^{14}C	‰	1987	175	20
Short	Δ^{14}C	‰	1805	0	5
Short	Δ^{14}C	‰	1910	-5	5
Short	Δ^{14}C	‰	1930	-12	5
Short	Δ^{14}C	‰	1950	-22	5
Trop.	δ^{13}C	‰	1987	-7.7	0.2
Deep	Δ^{14}C	‰	1973	-150	50
Mixed	Δ^{14}C	‰	1958	-58	10
Mixed	Δ^{14}C	‰	1973	110	50
Deep	ΣCO_2	moles m^{-3}	1973	2.34	0.06

Table 3: Other carbon cycle data used in the calibration of the model. For most of these data items (including all of the atmospheric ^{14}C data) the times refer to the middle of the year specified.

5 Results

5.1 'BASE' case results

The fit to the atmospheric CO_2 data is determined by the tuning of the initial CO_2 concentration, x_6 and the proportion of enhanced growth x_{23}. Figure 4 shows the fit that was achieved. The best-fit ^{14}C source strengths, x_{10} and x_{16}, are determined by the ^{14}C data. Figure 5 compares the tuned model output to the atmospheric ^{14}C data. Figure 6 shows the projected CO_2 concentrations for the BASE case; selected values are listed in Table 4.

The small Θ_{min} value of 9.5825 shows that the calibration data have been fitted well overall. The 'Suess effect' data from the Δ^{14}C of the terrestrial biota have the overall decline fitted well but the curvature is less than observed. (The calculated sequence is 1.5 -7.1, -13.2, -19.3 compared to 0, -5, -12, $-22‰$ for the short-lived biosphere in 1805, 1910, 1930, 1950). In the model the deep ocean is relatively ^{14}C-poor, with fitted Δ^{14}C of $-186.6‰$ compared to the datum $-150‰$. Similarly the post-bomb mixed layer Δ^{14}C is slightly low at 96‰ compared to 110‰ for 1973.

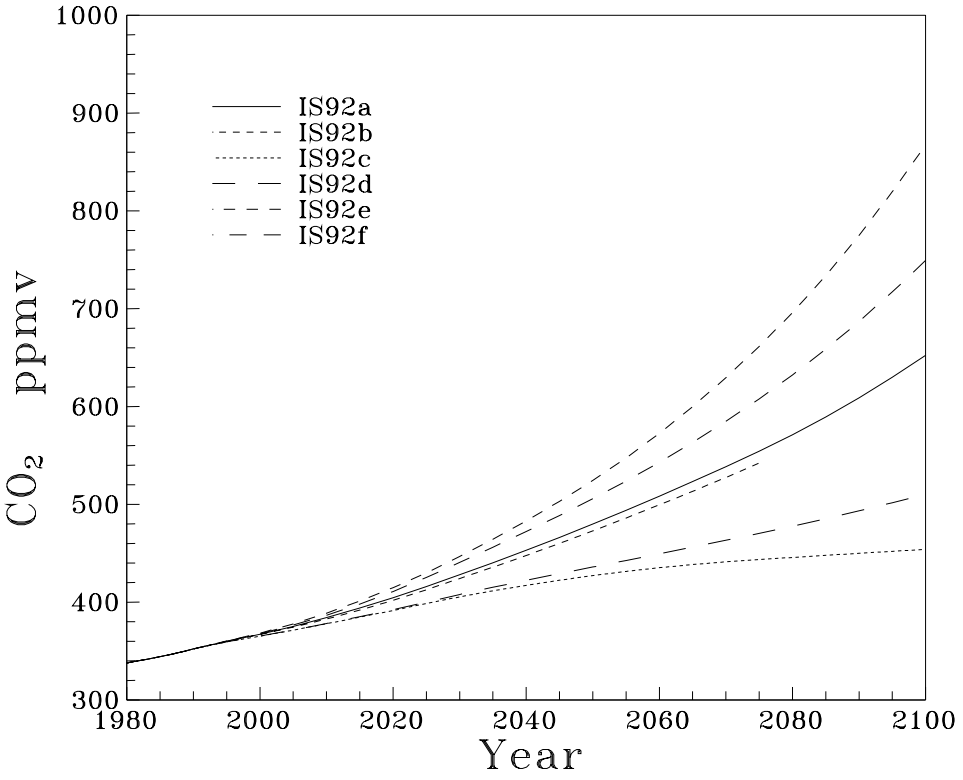

Figure 6: Projected CO_2 levels for each of the six release scenarios, using the BASE case set of parameters.

Scenario	1990	2000	2025	2050	2075	2100
IS92a	352.1	367.1	415.9	479.8	554.3	652.2
IS92b	352.1	367.0	412.7	472.8	542.1	—
IS92c	352.1	365.1	398.5	427.1	443.5	453.9
IS92d	352.1	365.3	400.0	435.9	470.3	510.2
IS92e	352.1	368.3	430.0	524.3	661.4	867.4
IS92f	352.1	367.7	425.3	505.7	607.8	749.3

Table 4: Projected CO_2 concentrations for the BASE case. Note that the dates refer to the beginning of the year.

5.2 Results from extended calibration ('FITTED' case)

Again, Table 1 lists the parameter values of the best 9-parameter fit that was obtained. Several important features of this case are:

- The vertical eddy-diffusion coefficient in the ocean is greater than in the BASE case, implying a greater oceanic uptake of CO_2.
- The proportion of the biota required to respond to excess CO_2 via 'CO_2-fertilisation' has decreased from 0.97 to 0.92.
- The fit to the deep ocean Δ^{14}C has improved and is $-169.3‰$ compared to the calibration value of $-150‰$ and the BASE case value of $-186.6‰$.

Table 5 shows the projections for the six IPCC (1992) scenarios at 25-year intervals for the FITTED case. These are so close to the BASE case that they are not plotted separately. Thus the inclusion of the isotopic data has served to confirm the responses derived using independent prior estimates rather than leading to large corrections to the parameter values.

Scenario	1990	2000	2025	2050	2075	2100
IS92a	352.1	367.1	415.7	479.4	553.6	650.9
IS92b	352.1	366.9	412.5	472.4	541.4	—
IS92c	352.1	365.4	398.4	426.8	443.1	453.2
IS92d	352.1	365.2	399.9	435.6	469.8	509.3
IS92e	352.1	368.3	429.8	523.8	660.3	865.4
IS92f	352.1	367.6	425.1	505.2	606.9	747.7

Table 5: Projected CO_2 concentrations for the FITTED case. Note that the dates refer to the beginning of the year.

5.3 Calibration uncertainty

Table 6 lists the results of a sequence of sensitivity studies using the Lagrange multiplier formalism described in section 4.1. The quantity Z whose range of variability is being considered is the projected CO_2 concentration in the year 2100, assuming scenario IS92a. We define a characteristic range by using the α values that approximately double the Bayesian sum-of-squares, Θ_{min} relative to the FITTED case, i.e. $\alpha = -0.7$ and 0.7. These span a range of 68 ppmv for the projected CO_2 concentration in 2100, i.e. a little over $\pm 10\%$ of the increase over the period 1990 to 2100. The $C(1986.5)$ and $C(1990)$ columns of Table 6 show that a significant part of the variability in the projections is associated with the flexibility that we permit in fitting the observed CO_2 data.

α	Θ_{min}	x_1	x_{23}	$C(1986.5)$	$C(1990)$	$C(2100)_a$
0.7	20.316	6405.6	0.66077	347.8	354.1	682.9
0.0	8.631	6245.2	0.91776	346.3	352.1	650.9
-0.7	20.798	7474.8	1.16266	344.7	349.9	614.8

Table 6: Sensitivity study for the projections to year 2100 using scenario IS92a. Note that the 1990 value refers to the beginning of the year.

5.4 Alternative atmospheric carbon budgets

In this section we present a series of calculations that further explore the range of uncertainty associated with the uncertainty in the current atmospheric carbon budget.

Firstly we consider the alternative estimates of the carbon releases arising from past land-use changes. Figure 3 shows the 'high' and 'low' estimates from Houghton (see appendix B), together with their average which we use in the FITTED and BASE cases. We have repeated the calculations performed for the FITTED case with the high and low release estimates, i.e. Bayesian re-calibration of the 9 parameters followed by the use of the best-fit parameters in constructing projections using each of the IPCC (1992) scenarios. The results are shown in the 'High Clearing' and 'Low Clearing' columns of Table 7.

Some of the key points of these results are:

- The range of past 'deforestation' estimates used here implies a corresponding range of about $\pm 10\%$ in the increase in atmospheric CO_2 over the period 1900 to 2100.
- The changes in the 'best-fit' parameters resulting from changes in the deforestation estimates mainly involve changing the fertilisation parameter. The 'best-fit' eddy diffusion changes little.
- The 'low release' estimates give the best fit.

- As might be expected, given that the net biotic changes will be very similar in each case, there is little effect on the initial δ^{13}C required in order to fit present-day observations.

	High Clearing	Low Clearing	Average	High Ocean	Low Ocean
x_1	6373.5	6038.3	6245.2	7966.4	4281.6
x_2	8.5608	8.5727	8.5780	8.3943	8.7776
x_5	2.8858	2.7107	2.7976	3.8344	1.7730
x_6	285.44	285.11	285.30	283.37	287.43
x_8	-6.4132	-6.4104	-6.4102	-6.395	-6.501
x_{10}	5.1628	5.1435	5.1549	5.2157	4.9863
x_{16}	2.8061	2.7793	2.7929	2.8458	2.6917
x_{17}	3.6985	3.6598	3.749	2.7159	2.9621
x_{23}	1.0634	0.7753	0.9177	0.7	1.2
Θ_{min}	10.352	7.4954	8.6306	13.5376	15.0742
$C(2100)_a$	623.4	671.4	650.9	664.3	634.3
$C(2100)_c$	444.4	463.2	453.2	459.1	445.7
$C(2100)_d$	497.9	522.3	509.3	517.4	499.3
$C(2100)_e$	838.3	894.9	865.4	884.7	841.2
$C(2100)_f$	724.9	772.7	747.7	764.1	727.2

Table 7: Effect of uncertainty in the atmospheric carbon budget upon the set of fitted parameters, and upon the CO_2 concentrations projected to 2100 for the 6 IPCC (1992) scenarios (suffices *a* to *f*). The FITTED case, using the average deforestation release, is in the column headed 'Average'. The effect of changing the deforestation estimates is shown by comparison with the columns 'High Clearing' and 'Low Clearing'. In these cases the data are fitted by the fertilisation adjusting to compensate for changes in the release. The oceanic uptake is essentially unchanged. The last two columns are from the runs described in Table 8, which use the average deforestation release and force high and low oceanic uptake by prescribing low and high values for CO_2-enhanced growth.

In order to explore a range of oceanic uptake rates, we have performed a sequence of calibrations using the average deforestation estimates to 1990 and fixing the fertilisation parameter x_{23} at a range of values from 0.6 to 1.3. The other 8 of the parameters adjusted in the FITTED case were tuned as before. The results are shown in Table 8 in which we list, for each prescribed value of x_{23}:

- The net changes in the two biotic reservoirs over the decade 1980–1990. (Note that in our formulation, deforestation only affects the long-lived component — we assume a rapid regrowth (or replacement growth) of the fast-turnover biotic component in cleared areas).
- The mean growth rate due to the fertilisation effect. This is obtained by taking the mean rate of change in biomass, i.e. $\frac{1}{10}$ of the sum of the biotic changes in the previous two columns, and adding back in the mean 1.740 Gt C y^{-1} release from land-use changes.

x_{23}	$\Delta N_{\rm L}$	$\Delta N_{\rm S}$	Growth	κ_b	x_1	x_8	$\Theta_{\rm min}$	$C(2100)_a$
0.6	-5.453	2.883	1.483	0.49	9282.1	-6.337	18.319	667.4
0.7	-3.356	3.326	1.737	0.58	7966.4	-6.395	13.538	664.3
0.8	-1.764	3.746	1.938	0.65	6921.7	-6.401	10.141	659.7
0.9	-0.157	4.126	2.136	0.72	6290.8	-6.417	8.254	652.2
1.0	1.420	4.479	2.330	0.78	5643.1	-6.431	8.093	645.6
1.1	2.961	4.861	2.552	0.84	4958.6	-6.450	9.438	639.7
1.2	4.470	5.217	2.709	0.90	4281.6	-6.501	12.296	634.3
1.3	5.732	5.516	2.869	0.95	4027.4	-6.499	16.316	625.6

Table 8: Investigations with systematic adjustment of terrestrial vs. marine sink produced by using average deforestation and prescribed CO_2-fertilisation. The changes in the biotic reservoirs are for the period 1980–1990. The 'Growth' column is the net biotic growth rate (in Gt C y^{-1}) due to the fertilisation effect, calculated as the average rate of change plus an average 1.740 Gt C y^{-1} mean net 'deforestation' rate. The biota-atmosphere growth ratio, κ_b is the ratio of the 'Growth' rate and the average 3 Gt C y^{-1} rate of growth of atmospheric carbon. (Note that $\Theta_{\rm min}$ excludes the term involving x_{23}).

- The biota-atmosphere growth ratio, κ_b. This is the ratio of the biotic growth rate from fertilisation to the rate of increase of atmospheric carbon (taken as 3.0 Gt C y^{-1}). Enting (1995) suggested that κ_b is a more appropriate measure of the CO_2-fertilisation effect than the traditional β-factor, in that κ_b is a measure of carbon storage which is what matters for atmospheric budget studies.

- The eddy diffusion parameter x_1, since this is the prime determinant of oceanic uptake in the model.

- The initial atmospheric δ^{13}C, x_8. This set of runs does imply differences in the δ^{13}C history between the different cases. The significance of these is discussed in Section 7.2 below.

- The objective function $\Theta_{\rm min}$. Note that in Table 8, $\Theta_{\rm min}$ is defined without a term $[(x_{23} - q_{23})/w_{23}]^2$ since x_{23} is not varied in these runs.

- The projected CO_2 concentration for the year 2100, assuming scenario IS92a.

We have given additional details of two of these cases, $x_{23} = 0.7$ and $x_{23} = 1.2$ in the final two columns of Table 7 where they can be compared to the results from alternative choices of deforestation scenario. For ease of comparision, all the $\Theta_{\rm min}$ values in Table 7 include the term $[(x_{23} - q_{23})/w_{23}]^2$.

The projections of CO_2 for the high ocean and low ocean uptake cases are shown in Figure 7. In addition, Figure 8 shows the fit to the atmospheric ^{14}C data for these same 2 cases. It will be seen that the differences for atmospheric ^{14}C are well within the uncertainties of the data.

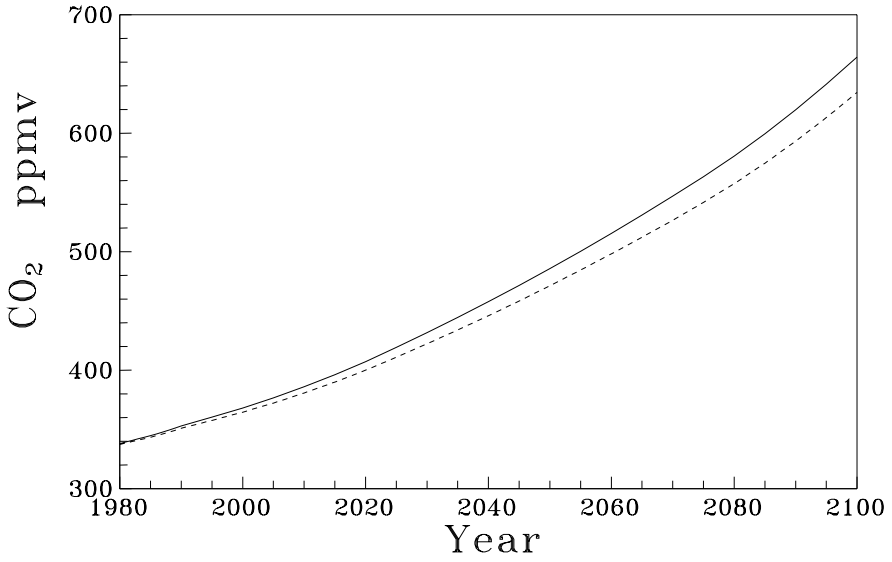

Figure 7: Range of projections, for the IS92a scenario, corresponding to the 'High ocean uptake' (solid) and 'Low ocean uptake' (dashed) cases from Table 7.

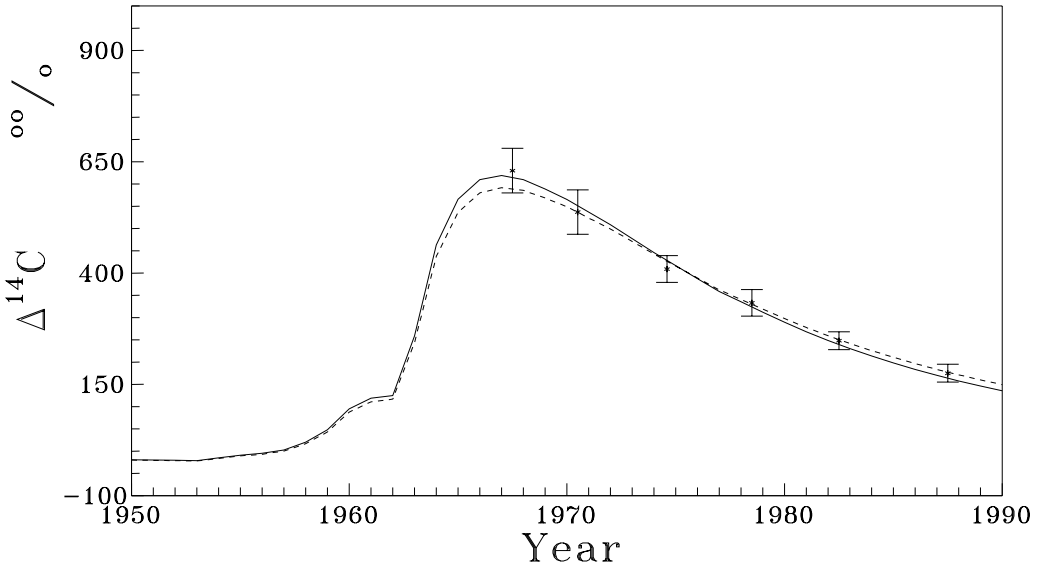

Figure 8: Range of fits to the atmospheric ^{14}C data corresponding to the 'High ocean uptake' (solid) and 'Low ocean uptake' (dashed) cases from Table 7. Calibration data as described for Figure 5.

6. Implications of carbon budget uncertainty

The results presented in the previous section reveal the considerable uncertainty in the role of the terrestrial biota in the current atmospheric carbon budget.

One of the major thrusts of recent carbon cycle research has been to use the spatial distribution of sources and sinks of atmospheric CO_2, as interpreted using atmospheric transport models, to constrain the range of possible source/sink strengths. Most recent estimates of the atmospheric carbon budget have drawn extensively on the constraints imposed by the spatial distributions of CO_2 (Keeling et al., 1989b; Tans et al., 1990; Sarmiento and Sundquist, 1992). Enting (1992b) has described a formalism for integrating the uncertainties from atmospheric transport modelling into atmospheric carbon budgets.

Some of the key results from transport modelling have been:

- Transport modelling indicates that the net tropical CO_2 source is lower than expected from the combination of ocean outgassing and deforestation. This seems to be a robust result, given by many modelling studies such as Pearman et al. (1983), Enting and Mansbridge (1989, 1991), Tans et al. (1989).
- Transport modelling indicates that the southern hemisphere sink is relatively low. Tans et al. (1990) used this result in their analysis that produced an estimate of 0.5 to 1.0 Gt C y^{-1} for the net global ocean sink. However, Enting and Mansbridge (1991) showed that atmospheric transport modelling of CO_2 without considering the role of CO would lead to an underestimate of the southern sink.

The preliminary assessment of the combined uncertainties in the global carbon budget by Enting (1992b) indicates that transport modelling can constrain the range of uncertainty obtained from direct estimates of the various sink strengths. The transport modelling studies can be effective in constraining regional budgets but appear to have little or no effect in reducing the uncertainties in global budgets. For the present study, the most important result is that the low tropical source estimated from transport modelling implies that deforestation is being offset by a 'fertilisation' effect. This is consistent with the need for a significant fertilisation component in the global model used here. Quantifying the constraints from transport modelling is complicated by the fact that the results are subject to restrictions on the achievable spatial resolution through the nature of the inversion problem (Enting, 1993).

7. Other Aspects of the Model Results

The purpose of this report is to document the application of the carbon cycle in the projection of future CO_2 concentrations resulting from the various emission scenarios defined in the IPCC (1992) report. However the calculations presented here raise several issues that are significant

for other studies of the carbon cycle. In this section we give a brief account of these, recognising that each deserves a more comprehensive study.

7.1 Atmospheric ^{14}C

Figure 5 compares the model calculations of atmospheric ^{14}C to two long sets of observational data, one in each hemisphere, plus recent data from Cape Grim, Tasmania. It will be seen that we obtain a very good fit over the period after nuclear weapons testing ceased but that the fit is poorer over the earlier period. A number of possible reasons for this are:

- Uncertainties in the strengths of bomb-sourced production. This is mainly due to the limited detail in information about energy yields. There are additional uncertainties due to (a) assigning to all types of detonation a single factor converting energy yield to ^{14}C production; (b) assigning only factors of 0.5 or 1 for surface vs. non-surface detonations.
- The injection of all ^{14}C into the stratosphere. This is reasonable for most of the tests but may give a noticable error for smaller, earlier tests which had lower altitudes of detonation and less fireball rise. This may contribute to the relatively poor simulation of the period of the nuclear test moratorium.
- The use of a single stratospheric reservoir (and single exchange time) for the injections of ^{14}C. The delayed rise in the calculated peaks, relative to the observations, suggests that a faster exchange rate might give a better fit and that perhaps a subdivision of the stratospheric reservoir might be appropriate. It is noted that the stratospheric mixing time is similar to its exchange time with the troposphere, and therefore that sparse stratospheric sampling can provide a misleading picture of stratospheric ^{14}C inventories (Lassey et al., 1990). This may explain why Enting and Mansbridge (1987b) could not obtain a good fit to the stratosphere-troposphere transport of ^{14}C from weapons testing, even with a much more detailed model.

In spite of the difficulties, we believe the fit to the observational data is extremely good. Since we are using a globally lumped model, we can not expect to fit the peaks, since at these times there was great spatial variability. Our representation of the period of the test moratorium (1960) is less satisfactory. Earlier attempts to use 1960 ^{14}C data in the calibration either failed to fit the data or distorted the overall fit. For the present, we attribute the problems to one or more of the model limitations listed above and so our calibration data set, as listed in Table 3, only uses atmospheric ^{14}C data from 1967 onwards.

7.2 Atmospheric ^{13}C

On several occasions in the preceding discussion, we have alluded to the role of ^{13}C data in providing additional information about the global carbon cycle. The stable isotope ^{13}C is subject

to different degrees of fractionation in air-sea exchange as opposed to uptake by the terrestrial biota. The study of atmospheric ^{13}C has been an important part of the CSIRO carbon cycle program. The main reason for including ^{13}C in the present calculations has been to explore the potential for using such data in refinements to the present calibration.

In previous carbon cycle studies, Enting and Pearman (1986, 1987) found that the current rate of change of atmospheric δ^{13}C did not provide additional constraints on the possible ambiguities in the atmospheric carbon budget — essentially the ^{13}C information duplicated the information contained in the atmospheric CO_2 data but with lower precision.

Another possibility is to consider the long-term change in atmospheric δ^{13}C. Early studies were based on the use of the δ^{13}C in tree-rings as a proxy for the atmosphere — as noted above this was found to be untenable. The recovery of air from bubbles trapped in polar ice provides an alternative opportunity for obtaining the history of changes in atmospheric δ^{13}C. Such data have been reported by Friedli et al. (1986). The comparisons presented in Tables 7 and 8 indicate the extent to which the change in atmospheric δ^{13}C can distinguish between the various cases. In each case, the calibration data has adjusted the intial δ^{13}C (i.e. x_8) so as to fit the 1987 atmospheric δ^{13}C. Thus differences in x_8 among the cases represent the extent to which the simulated change, δ^{13}C(1987) –δ^{13}C(1800) depends on the carbon budget in the model. Table 7 shows that this change in δ^{13}C is, as expected, primarily dependent on the balance between biotic exchange and ocean exchange. It is only minimally affected by the relative roles of fertilisation and clearing in determining the net biotic flux. The cases presented feature a change in the current biotic sink from near 0 up to 1 Gt C y^{-1} corresponding to differences of 0.1‰ in the δ^{13}C change over the last two centuries. Clearly if δ^{13}C data from ice-cores are to provide constraints on the carbon budget, then an improvement in precision is required.

7.3 Oceanic ^{13}C

Recently, Quay et al. (1992) have proposed an alternative way of using ^{13}C data to constrain the atmospheric carbon budget. They analyse the budget in terms of the releases S_f and S_r from fossil carbon and the terrestrial biota respectively and uptakes S_s and S_u by the ocean and biota respectively. The atmospheric carbon budget is expressed as

$$\int_{t_1}^{t_2} S_s(t)\,dt' = \int_{t_1}^{t_2} \left[S_f(t) + S_r(t) - S_u(t)\right]\,dt' - 12M[C(t_2) - C(t_1)] \qquad (7.1)$$

where $C(t)$ denotes the atmospheric CO_2 concentration and M is the number of moles of air in the atmosphere.

Defining the ocean carbon content as $T(t)$ then we can also write the integrated air-sea flux as

$$\int_{t_1}^{t_2} S_s(t)\,dt' = \int \left[T(t_2) - T(t_1)\right]\,dV \qquad (7.2)$$

where the volume integral is over all levels of the oceans in which significant change has occurred.

To consider ^{13}C we let R_f, R_r and R_u be the ^{13}C:(^{12}C+^{13}C) ratios in fluxes S_f, S_r and S_u respectively, and let R_a and R_s be the ^{13}C:(^{12}C+^{13}C) ratios of carbon in the atmosphere and oceans. The combination of (7.1) and (7.2) expresses the carbon budget without explicit reference to the air-ocean flux. The corresponding relation for ^{13}C is

$$\begin{aligned}
&\int_{t_1}^{t_2} \left[R_f(t)S_f(t) + R_r(t)S_r(t) - R_u(t)S_u(t)\right]\, dt - 12M\left[C(t_2)R_a(t_2) - C(t_1)R_a(t_1)\right] \\
&\qquad = \int \left[R_s(t_2)T(t_2) - R_s(T_1)T(t_1)\right]\, dV \\
&\qquad = \int \left[R_s(t_2)[T(t_2) - T(t_1)] + T(t_1)[R_s(t_2) - R_s(t_1)]\right]\, dV \\
&\qquad \approx \bar{R}_s(t_2) \int \left[T(t_2) - T(t_1)\right]\, dV + \bar{T}(t_1) \int \left[R_s(t_2) - R_s(t_1)\right]\, dV \qquad (7.3)
\end{aligned}$$

where the overbar denotes volume averages.

Using (7.2) to eliminate the terms involving change in ocean carbon and subtracting R_r times (7.1) gives equation (6) of Quay et al. (1992) in the form:

$$\begin{aligned}
&[\bar{R}_s(t_2) - R_r] \int_{t_1}^{t_2} S_s(t)\, dt \\
&\approx (R_f - R_r) \int_{t_1}^{t_2} S_f(t)\, dt + (R_u - R_r) \int_{t_1}^{t_2} S_u(t)\, dt - T(t_1) \int [R_s(t_2) - R_s(t_1)]\, dV \\
&\qquad -12MR_r[C(t_2) - C(t_1)] - 12M[C(t_2)R_a(t_2) - C(t_1)R_a(t_1)] \qquad (7.4)
\end{aligned}$$

The new data used by Quay et al. (1992) produces an estimate of the term $T(t_1) \int [R_s(t_2) - R_s(t_1)]\, dV$.

We have not attempted to reproduce the full ^{13}C budgeting calculation in the context of our model. We have merely examined our results to determine the extent to which changes in atmospheric and oceanic δ^{13}C might act as discriminators of the size of oceanic CO_2 uptake. The two cases that we consider are the high and low ocean uptake cases from Table 7, i.e. the x_{23} = 0.7 and 1.2 cases respectively from Table 8. We consider the change in δ^{13}C for the atmosphere and mixed layer over the period 1970–1990. For the low oceanic uptake case, the changes are -0.509 and $-0.289‰$, while for the high uptake case they are -0.549 and $-0.282‰$.

These results illustrate the point that in the Quay et al. analysis the role of the ocean δ^{13}C changes is not as a discriminator of oceanic uptake but rather as a contribution to 'close' the ^{13}C budget so that the atmospheric δ^{13}C changes can be used to discriminate between different oceanic CO_2 uptake rates. The sensitivity can be determined by looking at the extent to which $R_a(t_2)$ affects the expression (7.4).

7.4 Oceanic ^{14}C

In this section we explore the possibility that a more detailed description of oceanic ^{14}C could help constrain the oceanic uptake. Our main result is Figure 9 which shows a mean 1974 profile (the averaged GEOSECS data used by Siegenthaler and Joos, 1992) compared to the 3 cases 'High Ocean', 'Low Ocean' and 'Average' (i.e. the FITTED case) from Table 7. The spread in our calculated values is comparable to the observed spatial variability. This would suggest that effective use of additional ^{14}C data would require a disaggregated model. The one feature that seems to present scope for improvement within the scope of a globally-averaged ocean is a better representation of the depth of penetration of ^{14}C. In a number of recent modelling studies (e.g. Siegenthaler and Joos, 1992) a depth-dependent eddy-diffusion coefficient has been introduced to improve this aspect of the modelling.

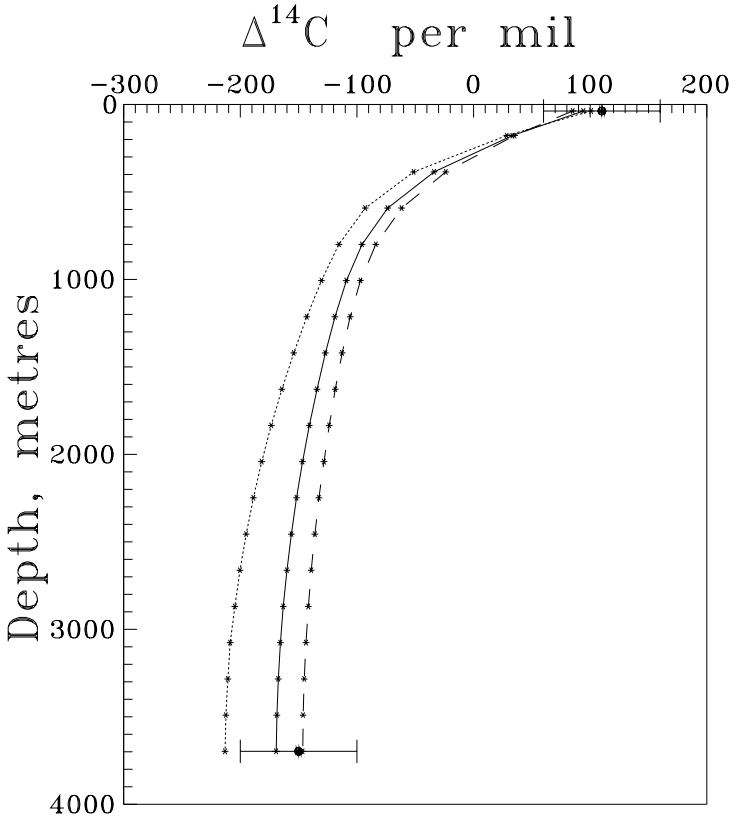

Figure 9: Calculated ocean profiles of Δ^{14}C for 1974 for the FITTED case (solid line), and the 'Low ocean uptake' (short dashes) and 'High ocean uptake' (long dashes) cases described in Table 7. Solid circles and ranges show our calibration data. Open circles and ranges show the calibration data used by Siegenthaler and Joos (1992).

8. Concluding Remarks

The main results of our calculations are the projected CO_2 concentrations shown in the figures and tables, reflecting the 'best-fit' calibration of our model and the ranges of uncertainty associated with various uncertainties in the modelling process.

One particular point to note is that the projected concentrations are significantly lower than the projections presented for the same set of scenarios by Wigley and Raper (1992). The results presented in Table 7 above would suggest that, compared to our calculations, they are using either a higher oceanic uptake or a lower 'deforestation' contribution. In addition, the predictions are sensitive to the current growth rate of CO_2. Table 6 shows the 1990 concentration which is a 3.5 year projection from the last data point fitted. The calculations by Wigley and Raper generally used larger values for the current rate of increase than those that we use (T. Wigley, personal communication). The differences may also reflect differing biotic formulations, particularly with respect to the correction defined by our equation (2.6).

Regardless of the reasons for the differences between our results and those of Wigley and Raper, it is clear that there is a need for careful definition of the methodology for modelling carbon changes in the terrestrial biota. The lack of specification in the 1990 scenarios, particularly the 'science' scenarios, prevented a consistent treatment of the terrestrial biota. Use of the 1992 scenarios will require a careful specification of which processes are prescribed and which are to be modelled. At the crudest level, this requires distinguishing between the 'gross' deforestation flux and the 'net' flux due to land-use change, but even more precise specification will probably be needed to ensure intercomparibility across a range of models.

Refinements to the carbon budgeting studies presented by Enting (1992b) will reduce the ranges of uncertainty that we have determined in this report. This will involve greater use of ^{13}C data and greater use of transport modelling with its associated uncertainty analysis. Such research is currently in progress.

Acknowledgements

This work was undertaken as part of the three-dimensional atmospheric transport modelling project funded by the State Electricity Commission of Victoria. The authors wish to thank Prof. T.M.L. Wigley for comments on the manuscript and for stimulating correspondence concerning equation 2.6. The printing of this report was funded by the Australian Department of the Environment, Sport and Territories as part of the Australian contribution to the work of the Intergovernmental Panel on Climate Change.

Notes on the electronic edition

The electronic edition was produced from the original LaTeX files by replacing the style for the old B5 format with the style for the CSIRO Atmospheric Research A4 technical paper format. As indicated by the erratum note inside the cover, the 1993 print edition had results for scenario IS92b which were incorrect after 2075. These have been deleted from Figure 6 and Tables 4, 5 and 7 in the electronic edition. References ‘in press’ or ‘submitted’ at the time of the print publication have been updated. Two footnotes have been added at points where we felt that the print version had been unclear.

References

Allen, L.H., Boote, K.J., Jones, J.W., Jones, P.H., Valle, R.R., Acock, B., Rogers, H.H. and Dahlman, R.C. (1987) Response of vegetation to rising carbon dioxide; photosynthesis, biomass and seed yield of soybean. *Global Biogeochemical Cycles* **1**, 1–14.

Bacastow, R.B. (1981) Numerical evaluation of the evasion factor. pp 95–101 of *Carbon Cycle Modelling: SCOPE 16.* Ed. B. Bolin. (John Wiley and Sons: Chichester).

Bolin, B. (Ed.) (1981) *Carbon Cycle Modelling: SCOPE 16.* (John Wiley and Sons: Chichester).

Broecker, W.S. and Peng, T.-H. (1992) Interhemispheric transport of carbon dioxide by ocean circulation. *Nature* **356**, 587–589.

Broecker, W.S., Gerard, R. and Ewing, M. (1960) Natural radiocarbon in the Atlantic ocean. *J. Geophys. Res.* **65**, 2903–2931.

Broecker, W.S., Peng, T.-H. and Engh, R. (1980) Modeling the carbon system. *Radiocarbon* **22**, 565–598.

Broecker, W.S., Peng, T.-S., Ostlund, G. and Stuiver, M. (1985) The distribution of bomb radiocarbon in the ocean. *J. Geophys. Res.* **90**, 6953–6970.

Brown, S., Gillespie, A.J.R. and Lugo, A.E. (1989) Biomass estimation methods for tropical forests with applications to forest inventory data. *Forest Science* **35**, 409–418.

CDIAC (1990) *Trends 90: A Compendium of Global Change.* Ed. T.A Boden, P. Kanciruk and M.P. Farrell. (Carbon Dioxide Information and Analysis Center: Oak Ridge).

CDIAC (1991) *Trends 91: A Compendium of Global Change.* Ed. T.A. Boden, R.J. Serpanski and F.W. Stoss. (Carbon Dioxide Information and Analysis Center: Oak Ridge).

Emanuel, W.R., Fung, I. Y.-S., Killough, G.G., Moore, B. and Peng, T.-H. (1985) Modeling the global carbon cycle and changes in the atmospheric carbon dioxide levels. pp141–173 of *Atmospheric Carbon Dioxide and the Global Carbon Cycle.* Ed. J.R. Trabalka. DOE/ER-0239. (U.S. Dept. of Energy: Washington).

Enting, I.G. (1982) *Nuclear Weapons Data for Use in Carbon Cycle Modelling.* Division of Atmospheric Physics, Technical Paper 44. (CSIRO, Australia).

Enting, I.G. (1985a) Principles of constrained inversion in the calibration of carbon cycle models. *Tellus* **37B**, 7–27.

Enting, I.G. (1985b) Green's functions and response functions in geochemical modelling. *PAGEOPH* **123**, 328–343.

Enting, I.G. (1990) Ambiguities in the calibration of carbon cycle models. *Inverse Problems* **6**, L39–L46.

Enting, I.G. (1991) *Calculating Future Atmospheric CO_2 Concentrations.* Division of Atmospheric Research Technical Paper No. 22. (CSIRO, Australia).
Electronic edition (2000) at *http://www.dar.csiro.au/publications/Enting_2000d.pdf*

Enting, I.G. (1992a) The incompatibility of ice-core CO_2 data with reconstructions of biotic CO_2 sources (II). The influence of CO_2-fertilised growth. *Tellus* **44B**, 23–32.

Enting, I.G. (1992b) *Constraining the Atmospheric Carbon Budget: A Preliminary Assessment.* Division of Atmospheric Research Technical Paper No. 25. (CSIRO, Australia).
Electronic edition (2000) at *http://www.dar.csiro.au/publications/Enting_2000b.pdf*

Enting, I.G. (1993) Inverse problems in atmospheric constituent studies. III: Estimating errors in surface sources. *Inverse Problems*, **9**, 649–665.

Enting, I.G. (1995) CO_2-climate feedbacks: Aspects of detection. pp313–329 of *Biotic Feed-*

backs in the Global Climate System: Will the Warming Feed the Warming? Ed. G.M. Woodwell and F.T, Mackenzie. (UP: New York). *Presented at IPCC workshop on Biotic feedbacks in the Global Climate System, Woods Hole, October, 1992.*

Enting, I.G. and Mansbridge, J.V. (1987) The incompatibility of ice-core CO_2 data with reconstructions of biotic CO_2 sources. *Tellus* **39B**, 318–325.

Enting, I.G. and Mansbridge, J.V. (1989) Seasonal sources and sinks of atmospheric CO_2: Direct inversion of filtered data. *Tellus* **41B**, 111–126.

Enting, I.G. and Mansbridge, J.V. (1991) Latitudinal distribution of sources and sinks of CO_2: Results of an inversion study. *Tellus* **43B**, 156–170.

Enting, I.G. and Newsam, G.N. (1990a) Inverse problems in atmospheric constituent studies: II. Sources in the free atmosphere. *Inverse Problems* **6**, 349–362.

Enting, I.G. and Newsam, G.N. (1990b) Atmospheric inversion problems: Implications for baseline monitoring. *J. Atmos. Chem.* **11**, 69–87.

Enting, I.G. and Pearman, G.I. (1982) *Description of a One-Dimensional Global Carbon Cycle Model.* Division of Atmospheric Physics, Technical Paper 42. (CSIRO, Australia).

Enting, I.G. and Pearman, G.I. (1983) *Refinements to a One-Dimensional Carbon Cycle Model.* Division of Atmospheric Research Technical Paper No. 3. (CSIRO, Australia).

Enting, I.G. and Pearman, G.I. (1986) The use of observations in calibrating and validating carbon cycle models. pp423–458 of *The Changing Carbon Cycle: A Global Analysis.* Ed. J. Trabalka and D. Reichle. (Springer-Verlag: New York.)

Enting, I.G. and Pearman, G.I. (1987) Description of a one-dimensional carbon cycle model calibrated using techniques of constrained inversion. *Tellus* **39B**, 459–476.

FAO (1990) *Interim report on Forest Resources Assessment 1990 Project.* FAO COFO-90/8(a) (FAO, Rome).

FAO (1991) *Second Interim Report on the State of Tropical Forests.* 10th World Forestry Congress, Paris, September, 1991.

Fearnside, P.M., Tardin, A.M. and Filho, L.G.M. (1990) *Deforestation rates in Brazilian Amazonia.* National Secretariat of Science and Technology, Brazilia. 8pp.

Flint, E.P. and Richards, J.F. (1994) Trends in carbon content in vegetation in South and Southeast Asia associated with changes in land use. pp201–209 of *Effects of Land Use Change on Atmospheric CO_2 Concentrations: Southeast Asia as a Case Study.* Ed. V.H. Dale. (Springer-Verlag: New York).

Friedli, H., Lötscher, H., Oeschger, H., Siegenthaler, U. and Stauffer, B. (1986) Ice core record of the $^{13}C/^{12}C$ ratio of atmospheric CO_2 in the past two centuries. *Nature* **324**, 237–238.

Francey, R.J. and Farquhar, G.D (1982) An explanation of $^{13}C/^{12}C$ variations in tree rings. *Nature* **297**, 28–31.

Gardner, R.H. and Trabalka, J.R. (1985) *Methods of Uncertainty Analysis for a Global Carbon Dioxide Model.* Publication DOE/OR/21400-4. (U.S. Dept. of Energy: Washington).

Gifford, R.M. (1993) Implications of CO_2 effects on vegetation for the global carbon budget. *Proceedings of the NATO ASI on The Global Carbon Cycle, Il Ciocco, September 1991.* Ed. M. Heimann. (Springer-Verlag: Berlin).

Hall, C.A.S. and Uhlig, J. (1991) Refining estimates of carbon released from tropical land-use change. *Canad. J. Forest Res.* **21**, 118–131.

Houghton, R.A. (1991) Tropical deforestation and carbon dioxide. *Climatic Change* **19**, 99–118.

Houghton, R.A. (1993) Changes in terrestrial carbon over the last 135 years. pp139–157 of

The Global Carbon Cycle. (Proceedings of the NATO ASI on The Global Carbon Cycle, Il Ciocco, September 1991). Ed. M. Heimann. (Springer-Verlag: Berlin).

Houghton, R.A. (1995) Effects of land-use change, surface temperature, and CO_2 concentration on terrestrial stores of carbon. pp333-350 of *Biotic Feedbacks in the Global Climate System: Will the Warming Feed the Warming?* Ed. G.M. Woodwell and F.T, Mackenzie. (UP: New York). *Presented at IPCC workshop on Biotic feedbacks in the Global Climate System, Woods Hole, October, 1992.*

Houghton, R.A. and Hackler, J.L. (1994) The net flux of carbon from deforestation and degradation in South and Southeast Asia. pp 301–307 of *Effects of Land Use Change on Atmospheric CO_2 Concentrations: Southeast Asia as a Case Study.* Ed. V.H. Dale. (Springer-Verlag: New York).

Houghton, R.A., Hobbie, J.E., Melillo, J.M., Moore, B., Peterson, B.J., Shaver, G.R. and Woodwell, G.M. (1983) Changes in the carbon content of terrestrial biota and soils between 1860 and 1980: A net release of CO_2 to the atmosphere. *Ecol. Monog.* **53**, 235–262.

Houghton, R.A., Boone, R.D., Fruci, J.R., Hobbie, J.E., Melillo, J.M., Palm, C.A., Peterson, B.J., Shaver, G.R., Woodwell, G.M., Moore, B., Skole, D.L. and Myers, N. (1987) The flux of carbon from terrestrial ecosystems to the atmosphere in 1980 due to land-use change: Geographic distribution of the global flux. *Tellus* **39B**, 122–139.

Houghton, R.A., Skole, D.L. and Lefkowitz, D.S. (1991) Changes in the landscape of Latin America between 1850 and 1980. *Forest Ecology and Management* **38**, 173–199.

IPCC (1990) *Climate Change: The IPCC Scientific Assessment.* Ed. J.T. Houghton, G.J. Jenkins and J.J. Ephraums for the Intergovernmental Panel on Climate Change. (CUP: Cambridge).

IPCC (1992) *Climate Change 1992: The Supplementary Report to the IPCC Scientific Assessment.* Eds. J.T. Houghton, B.A. Callender and S.K. Varkey for the Intergovernmental Panel on Climate Change. (CUP: Cambridge).

Keeling, C.D. (1973) Industrial production of carbon dioxide from fossil fuels and limestone. *Tellus* **25**, 174–198.

Keeling, C.D., Bacastow, R.B., Carter, A.F., Piper, S.C., Whorf, T.P., Heimann, M., Mook, W.G. and Roeloffzen, H. (1989a) A three-dimensional model of atmospheric CO_2 transport based on observed winds: 1. Analysis of observational data. In *Aspects of Climate Variability in the Pacific and Western Americas, Geophysical Monograph 55.* Ed. J.H. Peterson. (AGU: Washington).

Keeling, C.D., Piper, S. and Heimann, M. (1989b) A three-dimensional model of atmospheric CO_2 transport based on observed winds: 4. Mean annual gradients and interannual variations. In *Aspects of Climate Variability in the Pacific and Western Americas, Geophysical Monograph 55.* Ed. J.H. Peterson. (AGU: Washington).

Kohlmaier, G.H., Bröhl, H., Siré, E.O., Plöchl, M. and Revelle, R. (1987) Modelling stimulation of plants and ecosystem response to present levels of excess atmospheric CO_2. *Tellus* **39B**, 155–170.

Laurmann, J.A. and Spreiter, J.R. (1983) The effects of carbon cycle model error in calculating future atmospheric carbon dioxide levels. *Climatic Change* **5**, 145–181.

Lassey, K.R., Manning, M.R. and O'Brien, B.J. (1990) An overview of oceanic radiocarbon: its inventory and dynamics. *CRC Rev. in Aquatic Sciences* **3**, 117–146.

Lerman, J.C., Mook, W.G. and Vogel, J.C. (1970) C14 in tree rings from different localities. pp275–301 of *Radiocarbon Variations and Absolute Chronology.* Ed. I. Olsson. (John Wiley and Sons: New York).

Levin, I., Kromer, B., Schoch-Fischer, H., Bruns, M., Münnich, M., Berdau, D., Vogel, J.C. and Münnich, K.O. (1985) 25 years of tropospheric ^{14}C observations in central Europe. *Radiocarbon* **27**, 1–19.

Levin, I., Kromer, B. and Francey, R.J. (1990) Continuous measurements of ^{14}C in atmospheric CO_2 at Cape Grim. pp41–2 of *Baseline Atmospheric Program (Australia) 1988.* Ed. S.R. Wilson and G.P. Ayers. (Dept of Administrative Services and CSIRO: Australia).

Levin, I., Kromer, B. and Francey, R.J. (1991) Continuous measurements of ^{14}C in atmospheric CO_2 at Cape Grim. pp53–54 of *Baseline Atmospheric Program (Australia) 1989.* Ed. S.R. Wilson and J.L. Gras. (Dept of Administrative Services and CSIRO: Australia).

Liss, P.S. and Merlivat, L. (1986) Air-sea gas exchange rates: Introduction and synthesis. pp113–127 of *The Role of Air-Sea Exchange in Geochemical Cycling.* Ed. P. Buat-Menard. (Reidel, Hingham).

Machta, L., List, R.J. and Telegardas, K. (1963) Meteorology of fallout from the 1961–1962 nuclear tests. *Congress of the United States. Hearing Before Subcommittee in Research, Development and Radiation of the Joint Committee of Atomic Energy.* 88th Congress 46–61, June 1963.

Manning, M.R., Lowe, D.C., Melhuish, W.H., Sparks, R.J., Wallace, G. and Brenninkmeijer, C.A.M. (1990) The use of radiocarbon measurements in atmospheric studies. *Radiocarbon* **32**, 37–58.

Marland, G. and Boden, T. (1991) CO_2 emissions — Modern record. pp 386–389 of *Trends 91: A Compendium of Global Change.* Ed. T.A. Boden, R.J. Serpanski and F.W. Stoss. (Carbon Dioxide Information and Analysis Center: Oak Ridge).

Marland, G. and Rotty, R.M. (1984) Carbon dioxide from fossil fuels: A procedure for estimation and results for 1950–1982. *Tellus* **36B**, 232–261.

Marland, G., Boden, T.A., Griffin, R.C., Huang, S.F., Kanciruk, P. and Nelson, T.R. (1989) *Estimates of CO_2 Emissions from Fossil Fuel Burning and Cement Manufacturing Based on the United Nations Energy Statistics and the U.S. Bureau of Mines Cement Manufacturing Data.* Environmental Sciences Division Publication No. 3176. (Oak Ridge National Laboratory, Oak Ridge).

Martin, J.H., Knauer, G.A., Karl, D.M. and Broenkow, W.W. (1987) VERTEX: carbon cycling in the northeast Pacific *Deep Sea Res.* **34**, 267–285.

Nelder, J.A. and Mead, R. (1965) A simplex method for function minimization. *Computer J.* **7**, 308.

Myers, N. (1991) Tropical forests: present status and future outlook. *Climatic Change* **19**, 3–32.

Najjar, R.G., Sarmiento, J.L. and Toggweiler, J.R. (1992) Downward transport and fate of organic matter in the ocean: Simulations with a general circulation model. *Global Biogeochemical Cycles* **6**, 45–76.

Newsam, G.N. and Enting, I.G. (1988) Inverse problems in atmospheric constituent studies: I. Determination of surface sources under a diffusive transport approximation. *Inverse Problems* **4**, 1037–1054.

Nydal, R. and Lövseth, K. (1983) Tracing bomb ^{14}C in the atmosphere 1962–1980. *J. Geophys. Res.* **88C**, 3621–3642.

O'Brien, K. (1979) Secular variations in the production of cosmogenic isotopes in the earth's atmosphere. *J. Geophys. Res.* **84**, 423–431.

Oeschger, H., Siegenthaler, U., Schotterer, U. and Gugelmann, A. (1975) A box diffusion model to study the carbon dioxide exchange in nature. *Tellus* **27**, 168–192.

Pearman, G.I. (1980) Preliminary studies with a new global carbon cycle model. pp 79–91 of *Carbon Dioxide and Climate: Australian Research.* Ed. G.I. Pearman. (Australian Academy of Science: Canberra).

Pearman, G.I. and Hyson, P. (1986) Global transport and inter-reservoir exchange of carbon dioxide with particular reference to stable isotope distribution. *J. Atmos. Chem.* **4**, 81–124.

Pearman, G.I., Hyson, P. and Fraser, P.J. (1983) The global distribution of atmospheric carbon dioxide: 1. Aspects of observations and modelling. *J. Geophys. Res.* **88C**, 3581–3590.

Peng, T.-H., Broecker, W.S., Freyer, H.D. and Trumbore, S. (1983) A deconvolution of the tree ring based δ^{13}C record. *J. Geophys. Res.* **88C**, 3609–3620.

Press, W.H., Flannery, B.P., Teukolsky, S.A. and Vetterling, W.T. (1986) *Numerical Recipes: The Art of Scientific Computing.* (CUP: Cambridge).

Polglase, P.J. and Wang, Y.-P. (1992) Potential CO_2-enhanced carbon storage by the terrestrial biosphere. *Aust. J. Bot.* **40**, 641–656.

Quay, P.D., Tilbrook, B. and Wong, C.S. (1992) Oceanic uptake of fossil fuel CO_2: Carbon-13 evidence. *Science* **256**, 74–79.

Rau, G.H., Takahashi, T. and Des Marais, D.J. (1989) Latitudinal variations in plankton δ^{13}C: implications of CO_2 and productivity in past oceans. *Nature* **341**, 516–518.

Rau, G.H., Takahashi, T., Des Marais, D.J., Repeta, D.J. and Martin, J.H. (1992) The relationship between δ^{13}C of organic matter and [CO_2(aq)] in ocean surface water: data from a JGOFS site in the northeast Atlantic Ocean and a model. *Geochemica et Cosmochemica Acta* **56**, 1413–1419.

Robertson, J.E. and Watson, A.J. (1992) Surface thermal skin effect and the uptake of atmospheric CO_2 by the ocean. *Nature* **358**, 738–740.

Rotty, R.M. (1987) A look at 1983 CO_2 emissions from fossil fuels (with preliminary data for 1984). *Tellus* **39B**, 203–208.

Sarmiento, J.L. and Siegenthaler, U. (1992) New production and the global carbon cycle. pp317–332 of *Primary Productivity and Biogeochemical Cycles.* Ed. P.G. Falkowski and A.D. Woodhead. (Plenum: New York).

Sarmiento, J.L. and Sundquist, E.T. (1992) Revised budget for the oceanic uptake of anthropogenic carbon dioxide. *Nature* **356**, 589–593.

Setzer, A.W. and Pereira, M.C. (1991) Amazonia biomass burnings in 1987 and an estimate of their tropospheric emissions. *Ambio* **20**, 19–22.

Siegenthaler, U. and Joos, F. (1992) Use of a simple model for studying oceanic tracer distributions and the global carbon cycle. *Tellus* **44B**, 186–207.

Siegenthaler, U. and Oeschger, H. (1978) Predicting future atmospheric carbon dioxide levels. *Science* **199**, 388–395.

Siegenthaler, U. and Oeschger, H. (1987) Biospheric CO_2 emissions during the past 200 years reconstructed by deconvolution of ice core data. *Tellus* **39B**, 140–154.

Tans (1981) ^{13}C/^{12}C of industrial CO_2. pp 127–129 of *Carbon Cycle Modelling: SCOPE 16.* Ed. B. Bolin. (John Wiley and Sons: Chichester).

Tans, P.P., Conway, T.J. and Nakazawa, T. (1989) Latitudinal distribution of the sources and sinks of atmospheric carbon dioxide derived from surface observations and an atmospheric transport model. *J. Geophys. Res.* **94D**, 5151–5172.

Tans, P.P., Fung, I.Y. and Takahashi, T. (1990) Observational constraints on the global atmospheric CO_2 budget. *Science* **247**, 1431–1438.

Tarantola, A. (1987) *Inverse Problem Theory: Methods for Data Fitting and Model Parameter*

Estimation. (Elsevier: Amsterdam).
Wigley, T.M.L. and Raper, S.C.B. (1992) Implications for climate and sea level of revised IPCC emissions scenarios. *Nature* **357**, 293–300.

Appendix A: Description of the scenarios

The calculations described in this report use 6 different scenarios of future CO_2 emissions. These are prescribed in the IPCC (1992) supplement. For completeness, we reproduce a summary description of the scenarios and the assumptions on which they are based.

IS92a This is designed to update the 'business-as-usual' scenario from the IPCC (1990) report, in that the assumptions of qualitative changes are similar but revised numbers are used.

IS92b This is the same as IS92a except that those CO_2 reductions currently proposed by OECD countries are assumed to be implemented.

IS92c This uses lower estimates of population growth than the 'standard' case IS92a and also assumes a reduction in the cost of nuclear power. This is the only scenario in which CO_2 emissions do not continue to grow throughout the whole of the 21st century.

IS92d This assumes the same 'low' population growth as IS92c and assumes an early reduction in deforestation, in contrast to all the other scenarios which assume deforestation continues to the limit of available forests.

IS92e Like IS92a but asssuming a 'high' population growth and a complete phase-out of nuclear power.

IS92f Like IS92e, but with a reduction in nuclear power (due to price increase) rather than a complete phase-out.

Appendix B: The flux of carbon from changes in land use.

Contributed by R.A. Houghton

Ecologists have calculated the flux of carbon between terrestrial ecosystems and the atmosphere. Their approach is based on changes in land use and associated changes in vegetation and soil. The conversion of forests to agricultural lands, for example, releases carbon to the atmosphere through burning and decay and accumulates (seasonally) a small amount of carbon in the agricultural crop. Conversely, the regrowth of forests on abandoned agricultural lands withdraws carbon from the atmosphere and stores it again on land, in trees and soil. Current estimates of the flux of carbon from changes in land use vary between 0.6 and 2.5 Pg for 1980 (Houghton et al. 1987, Hall and Uhlig 1990, Houghton 1991) and between 1.1 and 3.6 PgC for 1990 (Houghton 1991), almost entirely from the tropics. It is important to note that this release of carbon includes the accumulation of carbon in forests regrowing after logging and after abandonment of agriculture. Land-use change includes reforestation as well as deforestation.

The high end of the range for 1990 now seems almost certainly too high. The increase between 1980 and 1990 was in large part due to an apparent increase in the rate of deforestation in the Brazilian Amazon (Myers 1991). Myers (1991) based his estimate of Brazilian deforestation on a study by Setzer and Pereira (1991), who used AVHRR data from the NOAA-7 satellite to determine the number of fires burning in Legal Amazonia (an area of 500 $\times 10^6$ ha including most of the Brazilian Amazon) during the dry season (mid-July through September). They accounted for the fact that some fires burned for more than one day (and should not be counted twice), and that a small, hot fire would saturate the entire pixel (1km square) and overestimate the area actually burned. With these adjustments, Setzer and Pereira (1991) estimated that about 20 $\times 10^6$ ha of fires burned in the Brazilian Amazon in 1987, about 60% of which, or 12 $\times 10^6$ ha, were on lands that had already been deforested. Their estimate of deforestation was 8 $\times 10^6$ ha.

Myers (1991) reduced their estimate to 5 $\times 10^6$ ha, to account for other factors. Nevertheless, even this reduced rate seems high according to more recent studies. Using data from Landsat (80m resolution rather than 1km resolution), the National Institute for Space Research (INPE) in Brazil found the rate of deforestation of closed forests in Brazil's Legal Amazonia to have averaged about 2.1 $\times 10^6$ ha yr-1 between 1978 and 1989 (Fearnside et al. 1990), about one fourth the rate initially determined by Setzer and Pereira (1991). The actual rate probably increased between 1978 and 1987, but fell substantially after 1987 to 1.8 $\times 10^6$ ha in 1988/89, to 1.38 in 1989/90, and to 1.11 in 1991. Recent work by Skole et al. (in press) shows rates similar to those reported by INPE.

When these more recent data from INPE are substituted for those reported by Myers (1991), the estimated rate of deforestation for all Latin America is revised from 7.7 to 4.5 $\times 10^6$ ha/yr. Over the 10-yr period 1980 to 1990, the rate of deforestation throughout the entire humid tropics now appears to have increased by about 40% rather than 90%. The revised estimate for the late 1980's is 10.66 $\times 10^6$ ha/yr for closed forests, alone. An independent estimate of the total rate for closed and open tropical forests is 17.1 $\times 10^6$ ha/yr (FAO 1990, 1991).

These revised rates of deforestation were used here with the data initially used by Houghton et al. (1991) to recalculate emissions of carbon from Latin America. The reanalysis omitted the conversion of forests to degraded land because that conversion is now thought to have been redundant with conversion of forest to shifting cultivation already included. The effect of both of these revisions was to reduce the calculated emissions from Latin America from about 0.7 PgC/yr (Houghton et al. 1991) to about 0.5 PgC/yr in 1980, and from about 0.9 to 0.7 PgC/yr in 1990.

Revisions were also made here to the data used to calculate the flux of carbon from tropical Asia and Africa. Rates of deforestation in Southeast Asia were revised upward recently by FAO (1990, 1991), and historical rates of degradation in the region were reassessed by Flint and Richards (1994). These revisions gave an estimate of flux for South and Southeast Asia that was about 0.7 PgC in 1990 (Houghton and Hackler, 1994). A reanalysis of land-use change in Africa, using lower estimates of biomass (Brown et al. 1989), gave an estimate of flux there of 0.35 PgC/yr in 1990.

As a result of these revisions, the global net flux is estimated to have been about 1.4 PgC in 1980 (1.3 Pg from the tropics and 0.1 Pg from outside the tropics) and 1.7 PgC in 1990 (essentially all of it from the tropics). The cumulative flux over the period 1850 to 1990 was 120 PgC. The accuracy of this estimate is not known. The estimate is about 15% lower than an earlier one (Houghton, 1993), with most of the difference occurring between 1985 and 1990. For South and Southeast Asia, the estimate is about 30% lower than an independent study (Richards and Flint, in press), and, for all the tropics in 1980, it is about 45% higher than the recent estimate by Hall and Uhlig (1990). Accuracy is estimated here to be better than $\pm$30%.

The revised estimate of flux from changes in land use (120 PgC over the period 1850–1990) is considerably higher than the estimate obtained from deconvolutions such as that of Siegenthaler and Oeschger (1987) and the temporal patterns of annual flux do not bear much resemblance. This is discussed further by Houghton (1993, 1995).

The tables list four sequences of estimates of net carbon flux associated with land-use change. These are the ‘low’ (Table 9) and ‘high’ (Table 10) estimates and their mean (Table 11), as used in the calculations in this report. These estimates reflect the information described in Houghton (1993).

The revised estimates (Table 12) take into account the issues discussed in this appendix. They became available too late for uses in the calculations presented in this report but have been adopted as ‘reference’ estimates for calculations being undertaken for inclusion in the proposed 1995 update to the IPCC scientific assessments.

	0	1	2	3	4	5	6	7	8	9
1850	0.4300	0.4300	0.4300	0.4300	0.4300	0.4400	0.4400	0.4400	0.4400	0.4400
1860	0.4400	0.4400	0.4500	0.4600	0.4700	0.4700	0.4700	0.4800	0.4900	0.5000
1870	0.5000	0.5000	0.5100	0.5200	0.5300	0.5300	0.5400	0.5400	0.5500	0.5600
1880	0.5700	0.5800	0.5800	0.5900	0.5900	0.6000	0.6000	0.6100	0.6100	0.6200
1890	0.6200	0.6200	0.6200	0.6100	0.6100	0.6100	0.6100	0.6100	0.6200	0.6200
1900	0.6200	0.6400	0.6600	0.6800	0.7000	0.7100	0.7100	0.7100	0.7000	0.7000
1910	0.7000	0.7000	0.6900	0.6800	0.6700	0.6700	0.6700	0.6800	0.6900	0.7000
1920	0.7000	0.7100	0.7200	0.7300	0.7400	0.7500	0.7400	0.7300	0.7200	0.7100
1930	0.7100	0.7100	0.7100	0.7000	0.7000	0.7000	0.6900	0.6800	0.6700	0.6700
1940	0.6700	0.6600	0.6500	0.6400	0.6300	0.6300	0.6500	0.6700	0.6800	0.6900
1950	0.7000	0.8000	0.9000	1.0000	1.1000	1.1000	1.1000	1.1000	1.1000	1.1000
1960	1.1000	1.1200	1.1500	1.1500	1.1700	1.2000	1.1700	1.1500	1.1500	1.1200
1970	1.1000	1.0700	1.0500	1.0500	1.0200	1.0000	1.0000	0.9900	0.9900	0.9800
1980	1.0580	1.1060	1.1530	1.2160	1.2790	1.3550	1.4310	1.5120	1.5940	1.6780
1990	1.7620	—	—	—	—	—	—	—	—	—

Table 9: ‘Low’ estimates of net carbon release from land-use change as used in this report.

	0	1	2	3	4	5	6	7	8	9
1850	0.4520	0.4640	0.4660	0.4670	0.4690	0.4710	0.4720	0.4740	0.4750	0.4750
1860	0.4920	0.4850	0.4920	0.5000	0.5080	0.5160	0.5220	0.5280	0.5340	0.5410
1870	0.5440	0.5530	0.5620	0.5660	0.5720	0.5790	0.5850	0.5890	0.5920	0.5940
1880	0.6210	0.6390	0.6580	0.6690	0.6790	0.6860	0.6920	0.6960	0.7000	0.7020
1890	0.7010	0.6940	0.6880	0.6830	0.6790	0.6760	0.6730	0.6720	0.6740	0.6760
1900	0.7320	0.7650	0.7910	0.8110	0.8280	0.8440	0.8510	0.8560	0.8600	0.8620
1910	0.8150	0.7880	0.7620	0.7600	0.7580	0.7500	0.7500	0.7490	0.7500	0.7510
1920	0.7890	0.8080	0.8230	0.8360	0.8420	0.8660	0.8750	0.8830	0.8660	0.8440
1930	0.8560	0.8610	0.8620	0.8600	0.8570	0.8520	0.8500	0.8490	0.8490	0.8500
1940	0.8390	0.8100	0.8080	0.8080	0.8120	0.8200	0.8300	0.8440	0.8610	0.8780
1950	0.9900	1.1500	1.2340	1.2940	1.4180	1.4820	1.5280	1.4780	1.4830	1.4880
1960	1.5730	1.6250	1.6630	1.7000	1.7350	1.7680	1.7470	1.7580	1.7750	1.7830
1970	1.6840	1.6690	1.6320	1.6090	1.5670	1.5950	1.6110	1.6310	1.6160	1.6090
1980	1.6930	1.7690	1.8450	1.9460	2.0460	2.1680	2.2900	2.4200	2.5500	2.6840
1990	2.8190	—	—	—	—	—	—	—	—	—

Table 10: ‘High’ estimates of net carbon release from land-use change as used in this report.

	0	1	2	3	4	5	6	7	8	9
1850	0.4410	0.4470	0.4480	0.4485	0.4495	0.4555	0.4560	0.4570	0.4575	0.4575
1860	0.4660	0.4625	0.4710	0.4800	0.4890	0.4930	0.4960	0.5040	0.5120	0.5205
1870	0.5220	0.5265	0.5360	0.5430	0.5510	0.5545	0.5625	0.5645	0.5710	0.5770
1880	0.5955	0.6095	0.6190	0.6295	0.6345	0.6430	0.6460	0.6530	0.6550	0.6610
1890	0.6605	0.6570	0.6540	0.6465	0.6445	0.6430	0.6415	0.6410	0.6470	0.6480
1900	0.6760	0.7025	0.7255	0.7455	0.7640	0.7770	0.7805	0.7830	0.7800	0.7810
1910	0.7575	0.7440	0.7260	0.7200	0.7140	0.7100	0.7100	0.7145	0.7200	0.7255
1920	0.7445	0.7590	0.7715	0.7830	0.7910	0.8080	0.8075	0.8065	0.7930	0.7770
1930	0.7830	0.7855	0.7860	0.7800	0.7785	0.7760	0.7700	0.7645	0.7595	0.7600
1940	0.7545	0.7350	0.7290	0.7240	0.7210	0.7250	0.7400	0.7570	0.7705	0.7840
1950	0.8450	0.9750	1.0670	1.1470	1.2590	1.2910	1.3140	1.2890	1.2915	1.2940
1960	1.3365	1.3725	1.4065	1.4250	1.4525	1.4840	1.4585	1.4540	1.4625	1.4515
1970	1.3920	1.3695	1.3410	1.3295	1.2935	1.2975	1.3055	1.3105	1.3030	1.2945
1980	1.3755	1.4375	1.4990	1.5810	1.6625	1.7615	1.8605	1.9660	2.0720	2.1810
1990	2.2905	—	—	—	—	—	—	—	—	—

Table 11: ‘Average’ estimates of net carbon release from land-use change as used in this report.

	0	1	2	3	4	5	6	7	8	9
1850	0.4357	0.4675	0.4824	0.4942	0.5040	0.5122	0.5189	0.5245	0.5296	0.5344
1860	0.5419	0.5336	0.5389	0.5440	0.5491	0.5544	0.5569	0.5604	0.5645	0.5688
1870	0.5718	0.5816	0.5877	0.5915	0.5958	0.6001	0.6049	0.6072	0.6089	0.6102
1880	0.6113	0.6422	0.6563	0.6629	0.6684	0.6728	0.6768	0.6777	0.6793	0.6790
1890	0.6872	0.6844	0.6850	0.6844	0.6833	0.6821	0.6804	0.6795	0.6812	0.6830
1900	0.6862	0.7485	0.7668	0.7817	0.7946	0.8060	0.8170	0.8221	0.8249	0.8270
1910	0.8283	0.7731	0.7572	0.7460	0.7435	0.7338	0.7372	0.7365	0.7360	0.7359
1920	0.7360	0.7846	0.7990	0.8110	0.8166	0.8274	0.8246	0.8243	0.8047	0.7804
1930	0.7747	0.7832	0.7786	0.7736	0.7677	0.7616	0.7674	0.7652	0.7616	0.7571
1940	0.7509	0.7300	0.7231	0.7161	0.7124	0.7094	0.7578	0.7682	0.7740	0.7759
1950	0.7824	0.9463	0.9872	0.9918	1.0885	1.1264	1.1551	1.0907	1.0828	1.0870
1960	1.0854	1.2317	1.2707	1.3092	1.3390	1.3627	1.3327	1.3323	1.3452	1.3500
1970	1.2972	1.2771	1.2459	1.2791	1.2595	1.2554	1.3386	1.3629	1.3628	1.4045
1980	1.4149	1.4351	1.4795	1.5098	1.5674	1.5959	1.6606	1.6942	1.7113	1.7053
1990	1.7129	—	—	—	—	—	—	—	—	—

Table 12: Revised estimates of net carbon release from land-use change, taking into account the issues raised in this report.

CSIRO Atmospheric Research Technical Papers

This series has been issued as *Division of Atmospheric Research Technical Paper* (nos. 1–19); *CSIRO Division of Atmospheric Research Technical Paper* (nos. 20–37) and *CSIRO Atmospheric Research Technical Paper* from no. 38.

Regular electronic publication commenced with no. 45. Earlier technical papers are progressively being made available in electronic form. A current list of technical papers, with links to available electronic versions, is maintained at *http://www.dar.csiro.au/info/TP.htm*.

Papers may be issued out of sequence. This list is current 2000/10/04.

No. 1 Galbally, I.E.; Roy, C.R.; O'Brien, R.S.; Ridley, B.A.; Hastie, D.R.; Evans, W.J.F.; McElroy, C.T.; Kerr, J.B.; Hyson, P.; Knight, W.; Laby, J.E. *Measurements of trace composition of the Austral stratosphere: chemical and meteorological data.* 1983. 31 p.

No. 2 Enting, I.G. *Error analysis for parameter estimates from constrained inversion.* 1983. 18 p.

No. 3 Enting, I.G.; Pearman, G.I. *Refinements to a one-dimensional carbon cycle model.* 1983. 35 p.

No. 4 Francey, R.J.; Barbetti, M.; Bird, T.; Beardsmore, D.; Coupland, W.; Dolezal, J.E.; Farquhar, G.D.; Flynn, R.G.; Fraser, P.J.; Gifford, R.M.; Goodman, H.S.; Kunda, B.; McPhail, S.; Nanson, G.; Pearman, G.I.; Richards, N.G.; Sharkey, T.D.; Temple, R.B.; Weir, B. *Isotopes in tree rings.* 1984. 86 p.

No. 5 Enting, I.G. *Techniques for determining surface sources from surface observations of atmospheric constituents.* 1984. 30 p.

No. 6 Beardsmore, D.J.; Pearman, G.I.; O'Brien, R.C. *The CSIRO (Australia) Atmospheric Carbon Dioxide Monitoring Program: surface data.* 1984. 115 p.

No. 7 Scott, John C. *High speed magnetic tape interface for a microcomputer.* 1984. 17 p.

No. 8 Galbally, I.E.; Roy, C.R.; Elsworth, C.M.; Rabich, H.A.H. *The measurement of nitrogen oxide (NO, NO_2) exchange over plant/soil surfaces.* 1985. 23 p.

No. 9 Enting, I.G. *A strategy for calibrating atmospheric transport models.* 1985. 25 p.

No. 10 O'Brien, D.M. *TOVPIX: software for extraction and calibration of TOVS data from the high resolution picture transmission from TIROS-N satellites.* 1985. 41 p.

No. 11 Enting, I.G.; Mansbridge, J.V. *Description of a two-dimensional atmospheric transport model.* 1986. 22 p.

No. 12 Everett, J.R.; O'Brien, D.M.; Davis, T.J. *A report on experiments to measure average fibre diameters by optical fourier analysis.* 1986. 22 p.

No. 13 Enting, I.G. *A signal processing approach to analysing background atmospheric constituent data.* 1986. 21 p.

No. 14 Enting, I.G.; Mansbridge, J.V. *Preliminary studies with a two-dimensional model using transport fields derived from a GCM.* 1987. 47 p.

No. 15 O'Brien, D.M.; Mitchell, R.M. *Technical assessment of the joint CSIRO/Bureau of Meteorology proposal for a geostationary imager/sounder over the Australian region.* 1987. 53 p.

No. 16 Galbally, I.E.; Manins, P.C.; Ripari, L.; Bateup, R. *A numerical model of the late (ascending) stage of a nuclear fireball.* 1987. 89 p.

No. 17 Durre, A.M.; Beer, T. *Wind information prediction study: Annaburroo meteorological data analysis.* 1989. 30 p. + diskette.

No. 18 Mansbridge, J.V.; Enting, I.G. *Sensitivity studies in a two-dimensional atmospheric transport model.* 1989. 33 p.

No. 19 O'Brien, D.M.; Mitchell, R.M. *Zones of feasibility for retrieval of surface pressure from observations of absorption in the A band of oxygen.* 1989. 12 p.

No. 20 Evans, J.L. *Envisaged impacts of enhanced greenhouse warming on tropical cyclones in the Australian region.* 1990. 31 p. [Out of print]

No. 21 Whetton, P.H.; Pittock, A.B. *Australian region intercomparison of the results of some general circulation models used in enhanced greenhouse experiments.* 1991. 73 p. [Out of print]

No. 22 Enting, I.G. *Calculating future atmospheric CO_2 concentrations.* 1991. 32 p.
Also electronic edition at *http://www.dar.csiro.au/publications/Enting_2000d.pdf*

No. 23 Kowalczyk, E.A.; Garratt, J.R.; Krummel, P.B. *A soil-canopy scheme for use in a numerical model of the atmosphere — 1D stand-alone model.* 1992. 56 p.

No. 24 Physick, W.L.; Noonan, J.A.; McGregor, J.L.; Hurley, P.J.; Abbs, D.J.; Manins, P.C. *LADM: A Lagrangian Atmospheric Dispersion Model.* 1994. 137 p.

No. 25 Enting, I.G. *Constraining the atmospheric carbon budget: a preliminary assessment.* 1992. 28 p.
Also electronic edition at *http://www.dar.csiro.au/publications/Enting_2000b.pdf.*

No. 26 McGregor, J.L.; Gordon, H.B.; Watterson, I.G.; Dix, M.R.; Rotstayn, L.D. *The CSIRO 9-level atmospheric general circulation model.* 1993. 89 p.

No. 27 Enting, I.G.; Lassey, K.R. *Projections of future CO_2.* with appendix by R.A. Houghton. 1993. 42 p.

No. 28 [Not published]

No. 29 Enting, I.G.; Trudinger, C.M.; Francey, R.J.; Granek, H. *Synthesis inversion of atmospheric CO_2 using the GISS tracer transport model.* 1993. 44 p.

No. 30 O'Brien, D.M. *Radiation fluxes and cloud amounts predicted by the CSIRO nine level GCM and observed by ERBE and ISCCP.* 1993. 37 p.

No. 31 Enting, I.G.; Wigley, T.M.L.; Heimann, M. *Future emissions and concentrations of carbon dioxide: key ocean/atmosphere/land analyses.* 1993. 120 p.

No. 32 Kowalczyk, E.A.; Garratt, J.R.; Krummel, P.B. *Implementation of a soil-canopy scheme into the CSIRO GCM – regional aspects of the model response.* 1994. 59 p.

No. 33 Prata, A.J. *Validation data for land surface temperature determination from satellites.* 1994. 36 p.

No. 34 Dilley, A.C.; Elsum, C.C. *Improved AVHRR data navigation using automated land feature recognition to correct a satellite orbital model.* 1994. 22 p.

No. 35 Hill, R.H.; Long, A.B. *The CSIRO dual-frequency microwave radiometer.* 1995. 16 p.

No. 36 Rayner, P.J.; Law, R.M. *A comparison of modelled responses to prescribed CO_2 sources.* 1995. 84 p.

No. 37 Hennessy, K.J. *CSIRO Climate change output.* 1998. 23 p.

No. 38 Enting, I.G. *Attribution of greenhouse gas emissions, concentrations and radiative forcing.* 1998. 27 p.
Also electronic edition at *http://www.dar.csiro.au/publications/Enting_2000c.pdf*

No. 39 O'Brien, D.M.; Tregoning, P. *Geographical distributions of occultations of GPS satellites viewed from a low earth orbiting satellite.* (1998) 28p.

No. 40 Enting, I.G. *Characterising the temporal variability of the global carbon cycle.* 1999. 53 p.
Also electronic edition at *http://www.dar.csiro.au/publications/Enting_2000a.pdf.*

No. 41 (in preparation).

No. 42 Mitchell, R.M. *Calibration status of the NOAA AVHRR solar reflectance channels: CalWatch revision 1.* 1999. 20 p.

No. 43 Hurley, P.J. *The Air Pollution Model (TAPM) Version 1: technical description and examples.* 1999. 41 p.
Also electronic edition at *http://www.dar.csiro.au/publications/Hurley_1999a.pdf*

No. 44 Frederiksen, J.S.; Dix, M.R.; Davies, A.G. *A new eddy diffusion parameterisation for the CSIRO GCM.* 2000. 31 p.

No. 45 Young, S.A. *Vegetation Lidar Studies.* Electronic edition in preparation.

No. 46 Prata, A. J. *Global Distribution of Maximum Land Surface Temperature Inferred from Satellites: Implications for the Operation of the Advanced Along Track Scanning Radiometer.* 2000. 30 p.
Electronic edition only. At *http://www.dar.csiro.au/publications/Prata_2000a.pdf*

No. 47 Prata, A. J. *Precipitable water retrieval from multi-filter rotating shadowband radiometer measurements.* 2000. 14 p.
Electronic edition only. At *http://www.dar.csiro.au/publications/Prata_2000b.pdf*

Address and contact details: CSIRO Atmospheric Research
Private Bag No.1 Aspendale Victoria 3195 Australia
Ph: (+61 3) 9239 4400; fax: (+61 3) 9239 4444
e-mail: chief@dar.csiro.au
http://www.dar.csiro.au.